Benzene and Toluene Biodegradation with Different Dissolved Oxygen Concentrations

by

Zhuolin Liu

A Thesis Presented in Partial Fulfillment
of the Requirements for the Degree
Master of Science

Approved November 2015 by the
Graduate Supervisory Committee:

Bruce E. Rittmann, Chair
Rosa Krajmalnik-Brown
Peter Fox

ARIZONA STATE UNIVERSITY

December 2015

ABSTRACT

This study reports on benzene and toluene biodegradation under different dissolved oxygen conditions, and the goal of this study is to evaluate and model their removal.

Benzene and toluene were tested for obligate anaerobic degradation in batch reactors with sulfate as the electron acceptor. A group of sulfate-reducing bacteria capable of toluene degradation was enriched after 252 days of incubation. Those cultures, originated from anaerobic digester, were able to degrade toluene coupled to sulfate reduction with benzene coexistence, while they were not able to utilize benzene. Methanogens also were present, although their contribution to toluene biodegradation was not defined.

Aerobic biodegradation of benzene and toluene by *Pseudomonas putida* F1 occurred, and biomass production lagged behind substrate loss and continued after complete substrate removal. This pattern suggests that biodegradation of intermediates, rather than direct benzene and toluene transformation, caused bacterial growth. Supporting this explanation is that the calculated biomass growth from a two-step model basically fit the experimental biomass results during benzene and toluene degradation with depleted dissolved oxygen.

Catechol was tested for anaerobic biodegradation in batch experiments and in a column study. Sulfate- and nitrate-reducing bacteria enriched from a wastewater treatment plant hardly degraded catechol within 20 days. However, an inoculum from a contaminated site was able to remove 90% of the initial 16.5 mg/L catechol, and Chemical Oxygen Demand was oxidized in parallel. Catechol biodegradation was inhibited when nitrite accumulated, presumably by a toxic catechol-nitrite complex.

The membrane biofilm reactor (MBfR) offers the potential for biodegrading benzene in a linked aerobic and anaerobic pathway by controlling the O_2 delivery. At an average benzene surface loading of 1.3 g/m^2-day and an average hydraulic retention time of 2.2 day, an MBfR supplied with pure O_2 successfully achieved 99% benzene removal at steady state. A lower oxygen partial pressure led to decreased benzene removal, and nitrate removal increased, indicating multiple mechanisms, including oxygenation and nitrate reduction, were involved in the system being responsible for benzene removal. Microbial community analysis indicated that *Comamonadaceae*, a known aerobic benzene-degrader and denitrifier, dominated the biofilm at the end of operation.

ACKNOWLEDGMENTS

I sincerely thank my advisor, Dr. Bruce E. Rittmann, for his constructive guidance and great help on my study and research. It has been the most wonderful experience working with him on such an interesting research topic during the last two years. His lessons on microbiology, bacterial energetics and kinetics, especially in biofilm area, gave me a deep understanding to environmental biotechnology. His comments and suggestions on my progress reports and thesis taught me skills for presenting my work. I also would like to thank my committee members Dr. Peter Fox and Dr. Rosa Krajmalnik-Brown for their time and expertise.

I appreciate all the help from people in Center for Environmental Biotechnology in Biodesign Institute, especially Dr. Chen Zhou, my research mentor, who taught me a lot on conducting research and gave me a lot of excellent advices on my thesis. I thank Dr. Aura Ontiveros for her help on reactor setup, taking bacterial sample, DNA extraction, and microbial community analysis. I owe thanks to Yen-jung Lai, Tengfei Chen, Michelle Young, Diana Calvo Martinez, Anca G. Delgado, Juan Maldonado, Joseph Miceli for their help on my research. I am grateful to my lab manager, Diane Hagner, for her support and regulation. It is a great pleasure for me to work with such a group of enthusiastic, friendly, bright scientists.

Last but not least, I would like to thank my parents, who brought me up, for always giving me great support and courage to study abroad.

TABLE OF CONTENTS

Page

LIST OF TABLES

LIST OF FIGURES

Figure Page

CHAPTER 1

INTRODUCTION AND BACKGROUND

1.1 Benzene Contamination in Groundwater

Benzene, also known as benzol, is a colorless liquid with a sweet odor. Benzene is volatile (12.7 kPa at 25˚C) and relatively soluble in water (1.79 g/L, 12˚C) compared to other hydrocarbons. In the environment, benzene is found in air, water and soil, and it mainly comes from industrial process and vehicle exhaust (World Health Organization, 1993). Today, benzene is commercially recovered from coal and petroleum sources. As of 2012, the global benzene production was approximately 43 million tonnes, and it ranks in the top 20 in production volume for chemicals produced in the United States (Merchant Reaearch & Consulting ltd, 2015).

Owing to its large production and high potential for mobility, benzene is one of the most prevalent organic contaminants in groundwater (Anderson & Lovley, 1997). Benzene is released to water from discharges of industrial wastewater, leachate from landfill, and gasoline leaks from underground storage tanks (Centers for Disease Control, 1994; Crawford et al., 1995; Staples et al., 1985). Benzene has been detected in groundwater samples collected at 832 of the 1,684 current and former NPL sites (U.S. Centers for Disease Control, 2007). The maximum benzene levels observed in monitoring wells in plumes from fuel spills at gasoline service stations ranged from 1,200 to 19,000 ppb (Salanitro, 1993).

Due to its toxicity and prevalence, it is of great health concern. Benzene exposure has been shown to result in decrease of blood-forming cells (Keller & Snyder, 1988), and it is associated with respiratory difficulties in children (Buchdahl et al., 2000; Delfino et

al., 2003; Nicolai et al., 2003). The U.S. EPA has set the maximum contaminant level (MCL) of benzene in drinking water at 5 μg/L, and the maximum contaminant level goal (MCLG) is zero (U.S. Environmental Protection Agency, 2009).

1.2 Benzene Biodegradation

1.2.1 Aerobic Biodegradation of Benzene

Aerobic biodegradation of benzene has been studied extensively. A study of aerobic degradation of benzene by the microbial population of industrial wastewater treatment units showed only 4 mg/L benzene remaining after 6 h with an initial dose of 50 mg/L (Davis et al., 1981). Chiang et al. (1989) showed that natural aerobic biodegradation was the major mechanism responsible for the soluble benzene reduction in the groundwater at a field site. Davis et al. (1994) observed rapid aerobic degradation of benzene in aquifer samples, with the time of 50% disappearance ranging from 4 to 14 days.

When oxygen is present, it not only serves as the terminal electron acceptor for respiration, but also takes part in initial enzymatic activation of the aromatic compound. The key feature of aerobic biodegradation of benzene, along with other aromatic compounds such as toluene, ethylbenzene, and xylene, is an initial "activation" of the aromatic ring by insertion of the element oxygen. Several such insertions lead to carboxylic acids or substituted pyrocatechols (Jindrova et al., 2002). Carboxylic acids and pyrocatechols can then be transformed to tricarboxylic acid cycle (TCA cycle) intermediates through ring cleavage, and the TCA cycle fully oxidized the intermediates into CO_2 and H_2O (Madigan et al., 2000; Rittmann, 1994; Rittmann & McCarty, 2001).

Many bacteria capable of aerobic growth on benzene degradation have been isolated (Gibson et al., 1968; Kukor & Olsen, 1991), including species of *Pseudomonas*,

Alcaligenes, *Nocardia*, and *Micrococcus*. *Pseudomonas* species are the most abundant (87% of identified benzene-degrading bacteria) and best studied group (Gibson et al., 1990; Ridgway et al., 1990). In this study, I selected *Pseudomonas putida* F1 for aerobic benzene biodegradation.

Two bacterial multi-component enzymatic systems, mono-oxygenases and di-oxygenases, are responsible for the initial transformation of the common aromatics benzene, toluene, ethylbenzene, and xylenes (BTEX), and several aerobic metabolic pathways have been identified (Gibson & Subramanian, 1984). Mono-oxygenases use only one oxygen atom from the oxygen molecule to attack aromatic ring, whose products are subsequently transformed to pyrocatechols, while di-oxygenases use two oxygen atoms to attack aromatic ring with the formation of 2-hydroxy-substituted compounds. Toluene degradation by *Pseudomonas putida* F1 follows the *tod* pathway (Figure 1), in which the aromatic ring is di-oxygenated first to form *cis*-toluene dihydrodiol and then it is dehydrogenated to form 3-methylcatechol (Gibson et al., 1970; Spain & Gibson, 1988). Benzene can be degraded by *P. putida* F1 via the same pathway and produces catechol (Spain et al., 1989).

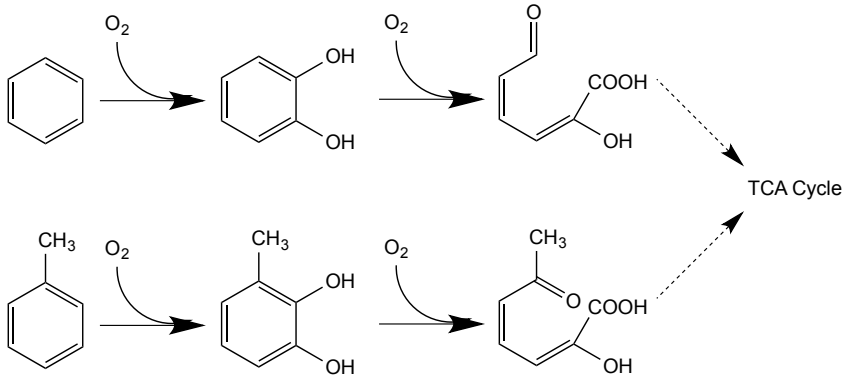

Figure 1. *P. putida* F1 catabolic pathways for benzene and toluene

1.2.2 Anaerobic Biodegradation of Benzene

In aquifers contaminated with organic matter continuously released from a point source, strongly reducing conditions develop close to the source, and the plume develops a series of redox zones along and transversal to the main groundwater flow direction (Christensen et al., 2000; Lovley, 2001). On the basis of Gibbs free energy for organic matter oxidation and when all electron acceptors are present, O_2 is used first, followed by NO_3^-, Mn, Fe, SO_4^{2-}, and finally methanogenesis or fermentation reactions (Christensen et al., 2001). As a result, benzene is often present in anoxic zones of aquifer environments (Lovley, 1997), and anaerobic bioremediation becomes a relevant groundwater remediation technique.

Aromatic compounds, such as benzene, are considered thermodynamically favorable electron donors for bacterial growth due to the high Gibbs free energy change of these compounds with all electron acceptors. However, benzene is regarded as recalcitrant under anoxic conditions (Colberg & Young, 1995), because its symmetrical ring structure features a stable π-electron cloud (Aihara, 1992) that has large (negative) resonance energy and thus resistant to cleavage (Gibson & Subramanian, 1984).

Although some research on anaerobic biodegradation of benzene in laboratory and aquifer field has been conducted, the majority of these published studies showed that anaerobic benzene biodegradation did not occur, and some of the studies suggested that anaerobic biodegradation of benzene might occur only when the incubation period is sufficiently long (320-520 days) (Aronson & Howard, 1997). Nonetheless, anaerobic biodegradation of benzene was observed in sediments, microcosms, column studies, microbial enrichments, and pure cultures with different electron acceptors, including

nitrate, sulfate, Fe(III), Mn(IV), (per)chlorate, and inorganic carbon in methanogenic condition (Weelink et al., 2010).

Several mechanisms are known for cleaving the aromatic ring anaerobically for aromatic compounds with functional groups such as carboxyl or hydroxyl groups. However, for benzene itself, the activation mechanism and further degradation steps are still unknown. Suggested initiation steps are hydroxylation (Chakraborty & Coates, 2005), carboxylation (Caldwell & Suflita, 2000), and methylation (Ulrich et al., 2005), followed by transformation to the central aromatic intermediates benzoyl-CoA, which is further degraded to CO_2.

1.2.3 Benzene Biodegradation in an Oxygen-Limiting Condition

In a contaminated aquifer, due to the redox gradient along the groundwater flow direction, O_2 usually is available only at low concentration at the fringe of the contaminant plume if the pristine aquifer contains significant amounts of dissolved oxygen (DO). Because O_2 is a key reactant in the first activation step for opening the aromatic ring, while microorganisms gain the most energy to support synthesis by using O_2 as a respiratory electron acceptor, aerobic biodegradation of benzene occurs widely when dissolved O_2 is available. According to stoichiometry, complete aerobic mineralization of 1 mg benzene requires approximately 1.4 mg O_2, which means the saturated DO level under ambient conditions (8-12 mg/L) is only sufficient for oxidation of 5-8 mg/L benzene. Often, the DO concentration often is well below saturation. Although addition of oxygen into the groundwater accelerates biodegradation, it is expensive. Thus, benzene biodegradation under oxygen-limiting conditions could be of great value to *in situ* bioremediation.

Benzene biodegradation has been shown to occur with micro-aerophilic conditions, e.g., at 0.05 mg/L DO, and catechol, phenol, and benzoate were detected as intermediates. No benzene biodegradation was observed in a strictly anoxic condition (Yerushalmi et al., 2001). Faster benzene degradation occurred when oxygen and nitrate were present together than with oxygen or nitrate alone (Majora et al., 1988). Aburto et al. (2009) reported benzene biodegradation by *in situ* anaerobic bacteria, but only when some oxygen was present; this suggests that the presence of some oxygen may be important for *in situ* benzene biodegradation.

When complete benzene biodegradation is feasible in the presence of a low DO level, the process probably features ring-activation by facultative micro-aerophiles (e.g., some *Pseudomonas* species), and then anaerobic oxidation of partially oxidized intermediates (e.g., catechol, benzoate, and phenol) is coupled with reduction of nitrate or sulfate as the respiratory electron acceptor. In this study, I designed a series of batch experiments and used a membrane biofilm reactor (MBfR) to monitor benzene biodegradation and microbial community with oxygen-limiting conditions that may follow this two-stage mechanism.

1.3 Review of O_2-based Membrane Biofilm Reactor

The membrane biofilm reactor (MBfR), an emerging technology for water and wastewater treatment, combines membrane technology with microbiology (Rittmann, 2007) and takes advantage of a natural partnership of membrane with biofilm (Rittmann, 2006). Biofilm grows on the outside wall of a bubble-less gas-transfer membrane, where pressurized gas diffuses from the interior lumen and is consumed by the biofilm on the outside. The MBfR has been used to treat a wide range of contaminants, including

organic and nitrogenous BOD when O_2 is delivered as an electron acceptor, although the most common application is reduction of oxidized contaminants when H_2 is supplied as an electron donor (Martin & Nerenberg, 2012).

The O_2-based MBfR (sometimes called a membrane aerated biofilm reactor, or MABR) was developed since the 1990s mainly for oxidation of organic BOD, nitrification (Syron & Casey, 2008), combined nitrification and denitrification (Timberlake et al., 1988), and anaerobic ammonia oxidation (Terada et al., 2007). In addition, it was applied for removal of specialized contaminants, such as benzene, by slow-growing, xenobiotic-degrading bacteria for petroleum-contaminated groundwater remediation (Martin & Nerenberg, 2012).

Compared to conventional bubble aeration, the O_2-based MBfR has several advantages: (1) bubble-less oxygen delivery offers high gas transfer rates and efficiency with consequent more energy savings, and it also prevents stripping of VOCs and greenhouse gases from liquid; (2) COD-removal rates can be controlled by adjusting the O_2 gas pressure; (3) COD and nitrogen can be simultaneously removed; and (4) biofilms formed adjacent to the membrane interface provide a natural shelter for slow-growing microorganisms.

1.4 Microbial Metabolism and Ecology in an O_2-based MBfR

In this study, O_2 not only serves as an electron acceptor and activator for aerobes, but also inhibits the activity of anaerobes. Membrane aeration seems an advantageous choice to control the redox condition in an MBfR, because I can easily and precisely control the O_2 delivery capacity and, thereby, the O_2 availability within the biofilm by adjusting O_2 gas pressure inside the hollow-fiber lumen.

MBfR biofilms behave different than conventional biofilms due to the counter-diffusional delivery of substrates, and they can also be different from each other as operational conditions changing. For conventional, co-diffusional biofilms (Figure 2a), the electron donor (benzene) and electron acceptor (O_2 and NO_3^-) concentrations are greatest at the outer edge of the biofilm. Under this scenario, aerobes may tend to live in the outer layer of the biofilm due to relatively abundant oxygen, using oxygen to activate or completely oxidize benzene. Intermediates may accumulate with oxygen depletion along the biofilm, and, without oxygen inhibition, anaerobes may tend to live in the inner layer of the biofilm, subsequently degrading those intermediates using nitrate as the electron acceptor.

For counter-diffusional biofilms, one substrate enters the biofilm from the bulk liquid, while the other is supplied from the hollow-fiber membrane. Figures 2b and c provide two examples: O_2-based MBfR biofilms conducting concurrent removal of benzene and nitrate with a limited O_2-supply and with a sufficient O_2-supply, respectively. Aerobes tend to live near to the membrane attachment surface, where O_2 is the most available, while anaerobes could be present in the outer layer of the biofilm; this is opposite to the conventional biofilm. When O_2 is not sufficiently provided from the membrane (Figure 2b), intermediates may accumulate with oxygen depletion and then be consumed within the anoxic biofilm with nitrate being the electron acceptor. When O_2 is well supplied from the membrane (Figure 2c), O_2 penetrates the biofilm, and benzene can be completely oxidized within the biofilm where aerobic bacteria are dominant.

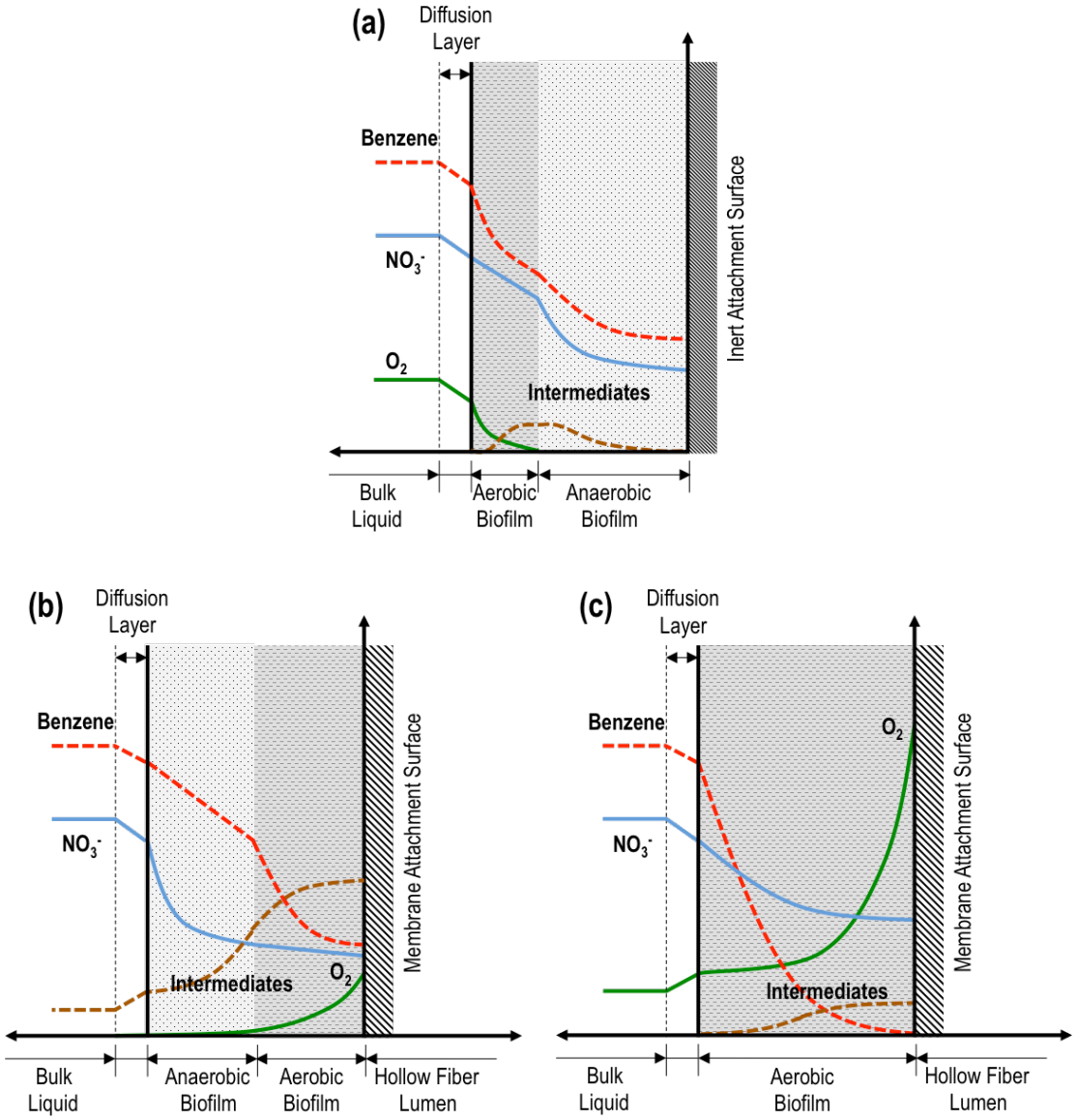

Figure 2. Schematic substrate gradients in biofilm. (a) Substrate gradients in a co-diffusional, conventional biofilm with limited dissolved-O_2 from the bulk liquid. (b) Substrate gradients in a counter-diffusional biofilm with limited O_2 supply. (c) Substrate gradients in a counter-diffusional biofilm with a sufficient O_2-supply.

1.5 Objective

The objective of this thesis is to evaluate benzene and toluene biodegradation under

strictly anoxic, fully aerobic, and O_2-limited conditions, and how they could be related to each other. My thesis consists of the following 5 parts:

1. I developed stoichiometry for benzene aerobic degradation to derive mathematical relationships among benzene (or toluene), O_2, and biomass. Based on the calculations, I also developed a mathematical model for substrate utilization, intermediates accumulation, and biomass growth.
2. I designed and carried out several batch experiments to test the biodegradability of benzene and toluene during anaerobic, sulfate reducing, aerobic, and micro-aerobic conditions.
3. I conducted a column study on catechol (an intermediate identified for benzene degradation under either aerobic or micro-aerobic condition) biodegradation coupled with nitrate and sulfate reductions by mixed cultures from a contaminated soil source.
4. I applied a bench-scale O_2-based MBfR to treat synthetic benzene-contaminated groundwater with different supplied O_2 partial pressures and, thus, delivery capacities.
5. I analyzed the microbial communities for the column and MBfR studies.

The remainder of this thesis is organized into six chapters. Chapter 2 describes the theoretical background of stoichiometry development and kinetic modeling. It also summarizes the materials and methods used commonly in these studies, including chemical analyses, physical properties, flux calculation, and bacterial sample preparation. Chapter 3 presents the anaerobic batch study and shows that toluene can be degraded by mixed cultures with sulfate reduction, while benzene is nearly unutilized. With obligate

anaerobic pathway being considered as an unpromising method for benzene biodegradation, Chapter 4 brings in oxygen as an alternative electron acceptor, and compares benzene and toluene degradation with aerobic and micro-aerobic batch conditions by a pure culture – *Pseudomonas putida* F1. It demonstrates the profound influence of oxygen on the biodegradation pathways and identifies catechol and 3-methylcatechol as the main intermediate metabolites of benzene and toluene transformation, respectively. As catechol showing accumulation during benzene biodegradation under oxygen-limiting condition, its further mineralization could be associated with anaerobic degradation. Thus, Chapter 5 documents catechol degradation coupled with nitrate or sulfate reducing in a series of batch experiments and a column study, and it further demonstrates the inhibition of complete catechol degradation by nitrite accumulation. In order to study the integrated DO concentration impacts on benzene biodegradation, Chapter 6 demonstrates benzene removal performance in an O_2-based MBfR reactor, which is able to easily adjust oxygen availability. It reveals that oxygen delivery determines the benzene and nitrate removal rates, as well as the biofilm community. Based on the observations and conclusions from previous chapters, Chapter 7 provides the overall conclusions and makes recommendations for promising future work.

CHAPTER 2

MATERIALS AND METHODS

2.1 Energy and Electron Balances for Oxygenation Reactions

The stoichiometry of biological reactions relies upon relationships describing energy and electron balances. Microorganisms transfer a portion of electrons (f_e^0) from their electron-donor substrate to an electron acceptor to generate energy (energy production), and they invest that energy to incorporate the other portion of electrons (f_s^0) into new microbial cells (cell synthesis).

For energy balance, the energy generated by transferring electrons from the donor to the acceptor must equal the energy invested to cell synthesis. Following Rittmann & McCarty (2001), the general relationship for the energy balance is:

$$A\varepsilon\Delta G_r + \Delta G_s = 0 \tag{1}$$

in which A is the equivalents of electron donor that must be oxidized to supply the energy required by synthesizing one equivalent of cells, ε is energy-transfer efficiency, ΔG_r is the free energy released per equivalent of donor oxidized, ΔG_s is the free energy to synthesize one equivalent of cells. Rearranging Equation (1) gives:

$$A = \frac{f_e^0}{f_s^0} = -\frac{\Delta G_s}{\varepsilon\Delta G_r} \tag{2}$$

For reactions involving intermediates formation or oxygenation reactions, not all the electrons in the electron-donor substrate are released to cell synthesis. Instead, some of the electrons are retained in the intermediates or transferred to molecular oxygen (Woo & Rittmann, 2000). For example, benzene is “activated” by inserting two oxygen atoms

during di-oxygenation where it releases two electrons, but reduction of two oxygen atoms requires four electrons; it needs invest of two electrons from inner electron carrier, although two carbons are oxidized to release two electrons in the end. As a result, oxygenation reactions do not yield a net release of electrons for energy-production or biomass synthesis, and this affects the energy and electron flows and, thereby, the overall stoichiometry.

Vanbriesen & Rittmann (2000) defined *T* as the fraction of electrons from the donor transferred to either the biomass synthesis pathways or energy generation, and *H* is the fraction of electrons held in intermediates. Furthermore, Woo & Rittmann (2000) defined *O* as the fraction of electrons from the donor transferred to molecular oxygen, and *R* is the fraction of electrons not sequestered in the intermediates. Thus, the electron balances for oxygenation reactions are given by:

$$T + H + O = 1 \tag{3}$$

$$R = T + O \tag{4}$$

$$f_s^0 + f_e^0 = T \tag{5}$$

Vanbriesen & Rittmann (2000) showed that Equation (2) and (5) could be solved simultaneously to obtain:

$$f_s^0 = \frac{T}{1+A} \quad \text{and} \quad f_e^0 = \frac{TA}{1+A} \tag{6}$$

In this case, the total donor equivalents used are the equivalents oxidized for energy generation plus one equivalent of cell synthesis, which is $1+A$. T can be computed by tracking electrons step by step for substrate half reaction. $R > T$ for reactions involving oxygenations, while $R = T$ for those not involving oxygenation.

The free energy of the energy-generation redox couple in Equation (1) and (2) is calculated as the difference between the free energy of the donor and acceptor half reactions:

$$\Delta G_r = \Delta G_a^{0'} - \Delta G_d^{0'} \tag{7}$$

in which $\Delta G_a^{0'}$ and $\Delta G_d^{0'}$ is the standard free energy for electron-acceptor half reaction and electron-donor half reaction, respectively. The overall free energy of the donor half reaction can be computed using the free energy of formations ($\Delta G_f^{0'}$) of all reactants and products in the half reaction (Equation 8). Some of the $\Delta G_f^{0'}$ values are tabulated in the literature and others could be estimated using group contribution theory (Mavrovouniotis, 1991; 1990).

$$\Delta G_d^{0'} = \sum \Delta G_f^{0'}(\text{products}) - \sum \Delta G_f^{0'}(\text{reactants}) \tag{8}$$

The free energy requirement for one equivalent of cell synthesis in Equation (1) and (2) can be calculated as the sum of the energy change resulting from the conversion of the carbon source to the common organic intermediates (ΔG_p), and the energy required to create and assemble cellular carbon (ΔG_{pc}) (Rittmann & McCarty, 2001). Here, pyruvate is the representative intermediates and ammonium is the nitrogen source. In sum, the equations can be written as:

$$\Delta G_p = 35.09 - \Delta G_c^{0'} \tag{9}$$

$$\Delta G_s = \frac{\Delta G_p}{\varepsilon^n} + \frac{\Delta G_{pc}}{\varepsilon} \tag{10}$$

in which 35.09 is the free energy of the half-reaction for pyruvate, $\Delta G_c^{0'}$ is the free

energy of the half-reaction for carbon source, ε is the energy-transfer efficiency, n accounts for energy generating ($n=-1$) or utilizing ($n=+1$) during conversion from the carbon source to the oxidation state of the common organic component (pyruvate here).

The full biodegradation stoichiometry (R_t) can be obtained by summation of the half reactions for electron-donor, electron-acceptor and cell synthesis via f_s^0 , f_e^0 , and T values (Vanbriesen & Rittmann, 2000):

$$R_t = f_e^0 \cdot R_a + f_s^0 \cdot R_c - T \cdot R_d \tag{11}$$

2.2 Biodegradation Kinetics Model

The relationship most frequently used to link substrate utilization and bacterial growth is the *Monod equation*, which relates the specific growth rate of bacteria to the concentration of rate-limiting substrate:

$$\mu_{syn} = \left(\frac{1}{X_a} \frac{dX_a}{dt} \right)_{syn} = \hat{\mu} \frac{S}{K+S} \tag{12}$$

in which μ_{syn} is the bacterial specific growth rate, X_a is the concentration of active biomass, $\hat{\mu}$ is the maximum specific growth rate, S is the substrate concentration, and K is the half-saturation constant. Equation (12) can be converted to a kinetic expression for the rate of substrate utilization rate:

$$r_{ut} = \frac{dS}{dt} = -\frac{\hat{q}S}{K+S} X_a \tag{13}$$

in which r_{ut} is the rate of substrate utilization, $\hat{q}$ is the maximum specific rate of substrate utilization. $\hat{q}$ and $\hat{\mu}$ are connected by true yield for cell synthesis (Y):

$$\hat{\mu} = Y \cdot \hat{q} \tag{14}$$

Previously, Yu et al. (2001b) developed a two-step model for the aerobic degradation of benzene and toluene by *Pseudomonas putida* F1. In the model, the first step is di-oxygenation, which transforms benzene and toluene into their catechol intermediates, but does not support biomass growth because it does not yield any electron equivalents that can be used to generate energy to support synthesis. The second step describes utilization of the catechol intermediates, whose oxidation generates electron equivalents and energy to support biomass synthesis. To represent the effects of the three substrate, (Dahlen & Rittmann, 2000) developed a multiplicative Monod expression was developed to describe the kinetics of the initial di-oxygenation reaction.

Because benzene and toluene are volatile, they can be present in liquid and gas phases. The microbial growth rate depends on the liquid-phase concentration, while the biomass yield depends on the total mass change of substrate. Thus, a modification term is needed to relate the total mass to the mass in the liquid phase:

$$m_t = m_l + m_g = m_l\left(1+\frac{HV_g}{V_l}\right) \tag{15}$$

where m refers to the mass of substrate in the gas phase (g), liquid phase (l), or the entire system (t). V_l is the liquid volume, V_g is the headspace volume, and H is the "dimensionless" Henry's law constant. The dimensional Henry's law constants for benzene and toluene are 5.55×10^{-3} and 6.64×10^{-3} atm-m^3/mol, respectively, and the "dimensionless" Henry's law constant is calculated using the universal gas constant of 0.082 atm/M-K and the temperature in Kelvin. If the temperature is 30°C, T is 303 K. Catechol intermediates are assumed to be present only in liquid phase due to their relatively low Henry's constants.

In a closed batch system, DO is only added to the aqueous phase by gas-liquid mass transfer from the headspace:

$$R_{O_2} = k_L a\left(S_O^* - S_O\right) \tag{16}$$

in which $k_L a$ is the volumetric mass transfer rate coefficient (T^{-1}), S_O is the dissolved oxygen concentration, and S_O^* is the liquid phase oxygen concentration in equilibrium with bulk gas phase O_2 content. In a closed batch system with oxygen consumption, S_O^* can change with time, making it is hard to estimate. If the oxygen mass transfer rate is much faster than biodegradation rate, S_0 never becomes small enough to limit the biotransformation kinetics.

2.3 Analytical Methods

Cell concentrations were measured as optical density at 600 nm (OD_{600}) with a Cary 50 UV-Visible Spectrophotometer (Varian, Inc., USA) and correlated to biomass concentration assayed as Volatile Suspended Solids (VSS). The carbon-free medium was used as optical density blanks for those experiments. A batch experiment for *Pseudomonas putida* F1 grown on pyruvate was designed to calibrate OD_{600} to biomass concentration. Each time for sampling, I took out 100-mL liquid sample and filtered it through a weighed standard glass-fiber filter for VSS measurement, and I took another 1-mL liquid sample for OD_{600} measurement. I measured VSS by drying the sample at 105°C for 1 hour and igniting it at 550°C for 20 minutes, according to the method 2540 E in *Standard Methods* (APHA 1999). Figure 3 shows the calibration curve, and the OD-mass correlation was linear up to 150 mg-VSS/L: 1.00 OD_{600} = 456.91 mgVSS/L.

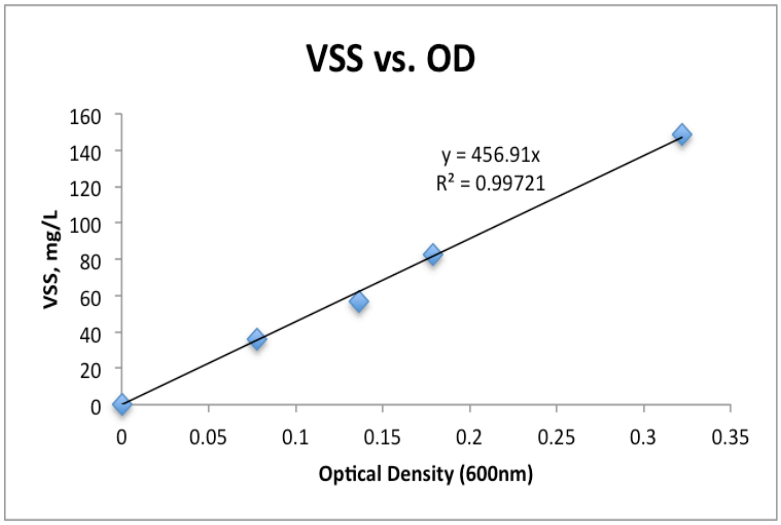

Figure 3. Calibration curve for volatile suspended solids to optical density at 600 nm.

Soluble benzene and toluene in aqueous samples were extracted by adding 1 mL of each aqueous sample and 1 mL of deionized water to 2 mL dichloromethane (DCM) and vortexing (VWR Analog Vortex Mixer, VWR International, Radnor, PA) the mixture for 30 min. The DCM layer was removed and filtered through a syringe filter with 0.2-µm pore-size PVDF membrane (Pall Life Sciences Acrodisc Syringe Filters, USA) and then stored at 4°C in 2-mL screw cap vials until analysis. Samples were analyzed using a Shimadzu gas chromatograph (GC-2010, Columbia, MD) equipped with a flame ionization detector (FID). The column and analytical conditions were as follows: Restek Rxi®-1HT chromatographic column with 30 m x 0.25 mm I.D. and 0.25 µm wall thickness; oven temperature program was 60°C with hold time 3 min; auto-sampler injection was 1 µL; carrier gas was H_2 at 3 mL/min; oxidizer was air at 400 mL/min; fuel was H_2 at 32 mL/min; and the temperatures of the injection port and the FID were 285°C and 315°C, respectively. The detection limit of this method for benzene and toluene was 5 µM.

Gas phase concentrations of benzene, toluene, and methane were quantified by

injecting 100 μL headspace samples with 250 μL gas-tight syringes (Hamilton Company, Reno, NV) into a Shimadzu gas chromatograph (GC-2010, Columbia, MD) equipped with a flame ionization detector (FID). The compounds were carried by hydrogen gas through an Rt^{TM}-QSPLOT capillary column (30 m×0.32 mm×10 μm, Restek, Bellefonte, PA). The oven temperature was maintained at 110°C for 1 min, followed by a temperature increase of 50°C min^{-1} to 200°C. Then, the temperature ramp was further raised to 240°C with a 15°C min^{-1} gradient and held for 2 mins. The temperatures of the FID and the injector were 240°C. The detection limit of this method for benzene and toluene was 0.5 μM.

Aqueous intermediates that formed during biodegradation experiments were detected by an Ultra-performance Liquid Chromatograph (UPLC; Waters, Milford, MA, USA) equipped with a 2.1×50 mm, 1.7-micron BEH C_{18} ACQUITY UPLC column. Samples were filtered with 0.2-μm pore-size PVDF membrane before injection into the column. The analytical method was modified from Yu et al. (2001a). The mobile phase was a 10 mM KH_2PO_4 buffer (pH 2.88) with an acetonitrile gradient from 10% to 30% in a flow rate of 0.4 mL/min. Solvents for UPLC analysis were of LC/MS grade. The detector was a photo diode array (PDA) with a detection wavelength of 207 nm. Samples (5 μL for each injection) were withdrawn automatically by the Sample Manager.

Nitrate, nitrite, and sulfate concentrations were measured with an ion chromatograph (Dionex ICS-2000) after the samples were filtered through 0.2-μm pore-size syringe filter (PVDF membrane, GE Healthcare Life Sciences Whatman^{TM}). The IC had an AG18 pre-column, an AS18 column, an eluent of 22 mM potassium hydroxide (KOH), and an eluent flow rate of 1 mL/min.

I measured DO using the Rhodazine D™ Method test kits (CHEMetrics K-7501, K-7599 and K-7512) with a range of 0.01 to 12 mg-O_2/L. Soluble chemical oxygen demand (sCOD) was measured with a HACH COD kit with a range of 20-1500 mg/L. For the sCOD test, 2 mL of filtered sample (0.2-μm) were added to the vial containing digestion solution, digested at 150 ˚C for 2 h, and then assayed for absorbance after cooling following Hach's standard method. I measured pH with a pH probe (Thermo Electron Corporation) and alkalinity by a HACH alkalinity kit with a range of 25-400 mg $CaCO_3$/L.

2.4 Electron Equivalents and Fluxes Calculation

I calculated the electron equivalents of any substrate based on assuming full oxidation or reduction. For instance, 1 mole benzene equals 1×30 = 30 e^- equivalents (assuming full oxidation to CO_2), 1 mole nitrate equals 1×5 = 5 e^- equivalents (assuming reduction from NO_3^- to nitrogen gas), 1 g COD equals 1/32×4 = 0.125 e^- equivalents.

I calculated benzene, NO_3^-, and sCOD removal fluxes (e^- mEq/m^2-day) based on equation (17):

$$J = \frac{Q \times (S^0 - S)}{A} \tag{17}$$

in which J is the flux (e^- mEq/m^2-day), Q is the influent volumetric flow rate (L/day), S^0 and S are the influent and effluent concentration, respectively, and A is the membrane surface area (m^2). The maximum O_2 delivery capacity (e^- mEq/m^2-day) was calculated according to Tang et al. (2012).

2.5 Microbial Sampling and Analysis

At the end of MBfR operation, I took a biofilm sample by scratching 1.5-cm biofilm from a single hollow-fiber membrane, as described by Ontiveros-Valencia et al. (2012). I extracted the biofilm's DNA by following the directions of the manufacturer (Qiagen, USA). At the beginning and the end of the column study on catechol anaerobic degradation, I took bacterial samples by making pellets from suspension liquid. I extracted the biomass pellets' DNA by following the manufacturer of PowerMax® soil DNA Isolation Kit (MO BIO Laboratories, Carlsbad, CA, USA). All the DNA samples were stored at -80 ˚C until shipping for 454 pyrosequencing.

I performed amplicon sequencing of the V4 region of the 16S rRNA gene using the barcoded primer set 515F/806R (Caporaso et al., 2012). Library preparation was performed at the Microbiome Analysis Laboratory in the Swette Center for Environmental Biotechnology (http://krajmalnik.environmentalbiotechnology.org /microbiome-lab.html). The library preparation was according to the protocol from Earth Microbiome Project. Sequencing was performed in a MiSeq Illumina sequencer (Illumina Inc., USA) using the chemistry version 2 (2x150 paired-end). Raw sequences were processed using the QIIME 1.9.0 suite (Caporaso et al., 2010), as explained in detail in Ontiveros-Valencia et al. (2014).

CHAPTER 3

ANAEROBIC BENZENE AND TOLUENE DEGRADATION LINKED TO SULFATE REDUCTION

3.1 Experimental Setup

I ran a batch test for benzene and toluene biodegradation using anaerobic serum bottles with an inoculum of fresh sludge from an anaerobic digester (Mesa Northwest Water Reclamation Plant, City of Mesa, AZ).

Bacteria were first enriched anaerobically on pyruvate with sulfate as the electron acceptor, and then they were transferred directly to batch experiments. I prepared two 240-ml serum bottles with inoculum (labeled as 'SL1' and 'SL2') and another serum bottle without inoculum as a control (labeled as 'Control'). In the glove box, each bottle was filled with 140-ml anoxic medium modified from Dou et al. (2008a) and sealed with a rubber stopper and an aluminum crimp, and then taken out for autoclaving. The medium was composed of (in g/L) 0.1 $MgCl_2$, 0.1 $CaCl_2$, 1 NH_4Cl, 1 K_2HPO_4, 2 Na_2SO_4, and 1 mL of trace mineral solution. The trace minerals solution consisted of (mg/L): 100 $ZnSO_4$-$2H_2O$, 30 $MnCl_2$-$4H_2O$, 300 H_3BO_3, 200 $CoCl_2$-$6H_2O$, 10 $CuCl_2$-$2H_2O$, 10 $NiCl_2$-$6H_2O$, 30 Na_2MoO_4-$2H_2O$, and 30 Na_2SeO_3 (Chung et al., 2006). The pH in the medium was 6.95.

Pure benzene and toluene were directly injected into the serum bottles using gas-tight syringes. The serum bottles were then maintained at 30°C on a shaker table for at least 48 hours to allow equilibrium of benzene and toluene partitioning between the liquid and gas phase. The actual initial concentrations of benzene dissolved in liquid phases of SL1 and SL2 were 241 and 145 mg/L, respectively. The actual initial

concentrations of toluene dissolved in liquid phases of SL1 and SL2 were 16 and 70 mg/L, respectively. The initial sulfate concentration was 1227 mg/L, which was set up enough for complete oxidations of benzene and toluene according to stoichiometry.

I inoculated the SL1 and SL2 bottles with the inoculum mentioned before, and all the three bottles were then incubated upside-down on a shaker table at a constant temperature of 30°C. At each sampling point, I measured benzene, toluene and methane concentrations in headspaces, as well as optical density (OD_{600}) and sulfate concentrations in liquid by those methods described in chapter 2.

3.2 Results and Discussion

Figure 4 presents the total mole masses of benzene, toluene, and methane and the concentration of sulfate during 281 days. The differences among bottles for the actual initial benzene and toluene concentrations probably were due to their high volatilities or small amount of injection volume (30 μL), which may have caused deviations from the target concentrations. As a result, SL1 and SL2 turned out to be two distinguishable conditions rather than duplicates. These concentrations should not be toxic to the microorganisms according to experiments conducted by others (Beller et al., 1992; Dou et al., 2008b; Shim et al., 2005).

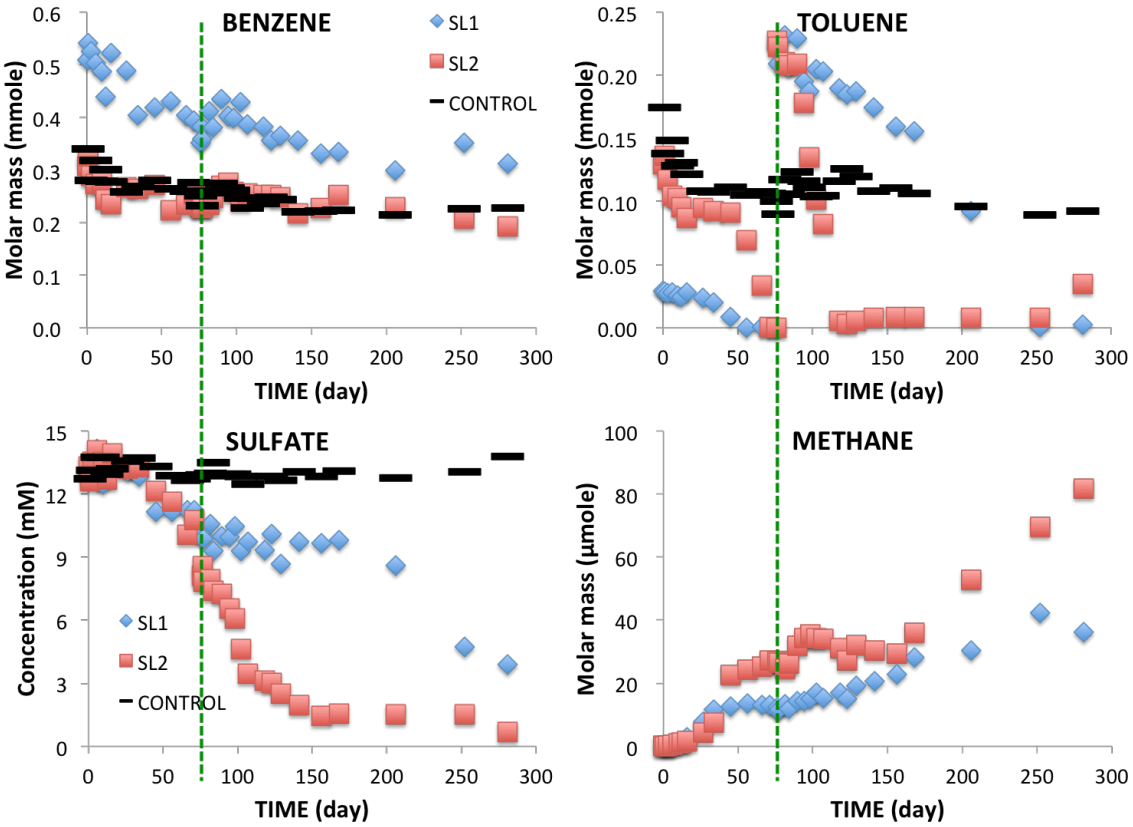

Figure 4. Total mole masses of benzene, toluene, and methane and concentrations of sulfate in the inoculated bottles SL1 (◆) and SL2 (■) plus a control bottle (−) without inoculum. The green dashed lines show when I re-spiked toluene to ~130 mg/L at Day 76.

During the first 10 days, toluene concentrations decreased by 20% and 30% in SL2 and control, respectively, without corresponding sulfate decrease or methane accumulation in SL2. Benzene had similar trends. Thus, rather than biodegradation, the loss in aqueous-phase concentration probably was due to the extended time needed to stabilize toluene partitioning among different phases (gas, liquid and adsorbed), especially for the higher concentration.

After a lag time of 20 to 30 days, toluene consumption along with sulfate decrease and methane production took place in SL1 and SL2, and toluene was completely removed within 50 days and 70 days, respectively. As of Day 76, the benzene concentration

remained stable in SL2, although it decreased by 23% in SL1, including the non-biodegradation loss mentioned above. Benzene is regarded as more recalcitrant under anoxic conditions than toluene, with anaerobic biodegradation of benzene occurring only after the anaerobic biodegradation of toluene (Foght, 2008).

On Day 76, I re-spiked SL1 and SL2 with toluene (to ~130 mg/L in both bottles), and observed the anticipated steady biodegradation of toluene. Toluene was completely degraded within 176 days (by Day 252) and 42 days (by Day 118) after re-spiking in SL1 and SL2, respectively. The difference between the toluene utilization rates in these two experiments was probably due to different abundances of capable microorganisms. On the one hand, perhaps due to more biomass synthesis with the relatively higher toluene concentration, the culture in SL2 (initially had 70 mg/L toluene) was able to utilize toluene spiked at ~130 mg/L faster than the culture adapted to relatively lower concentration (~16 mg/L in SL1). On the other hand, some loss of active biomass was possible in SL1, since toluene was re-spiked 20 days after it had been completely removed from SL1, while toluene was re-spiked immediately after its complete degradation in SL2. Sulfate decreases corresponded to toluene degradation, and sulfate was reduced faster in SL2 than in SL1.

After 281 days of incubation, benzene decreased by 40%, 33%, and 28% in SL1, SL2, and control, respectively. These similar declines point to little benzene biodegradation occurring in SL1 and SL2. In SL2, the small amount of benzene degradation slowly occurred after toluene was depleted. Accordingly, sulfate was stable around 1.5 mM after toluene was biodegraded, which further supports that benzene was hardly biodegraded by sulfate reduction.

Methanogenesis took place immediately after inoculation, and methane gradually accumulated. However, methane production was inhibited by sulfate reduction. In SL2, methane showed faster accumulation with relatively slower sulfate utilization at the beginning and after Day 150. This correspond to the Gibbs free energy for organic matter oxidation described in Chapter 1, which shows sulfate was a more favorable electron acceptor than inorganic carbon.

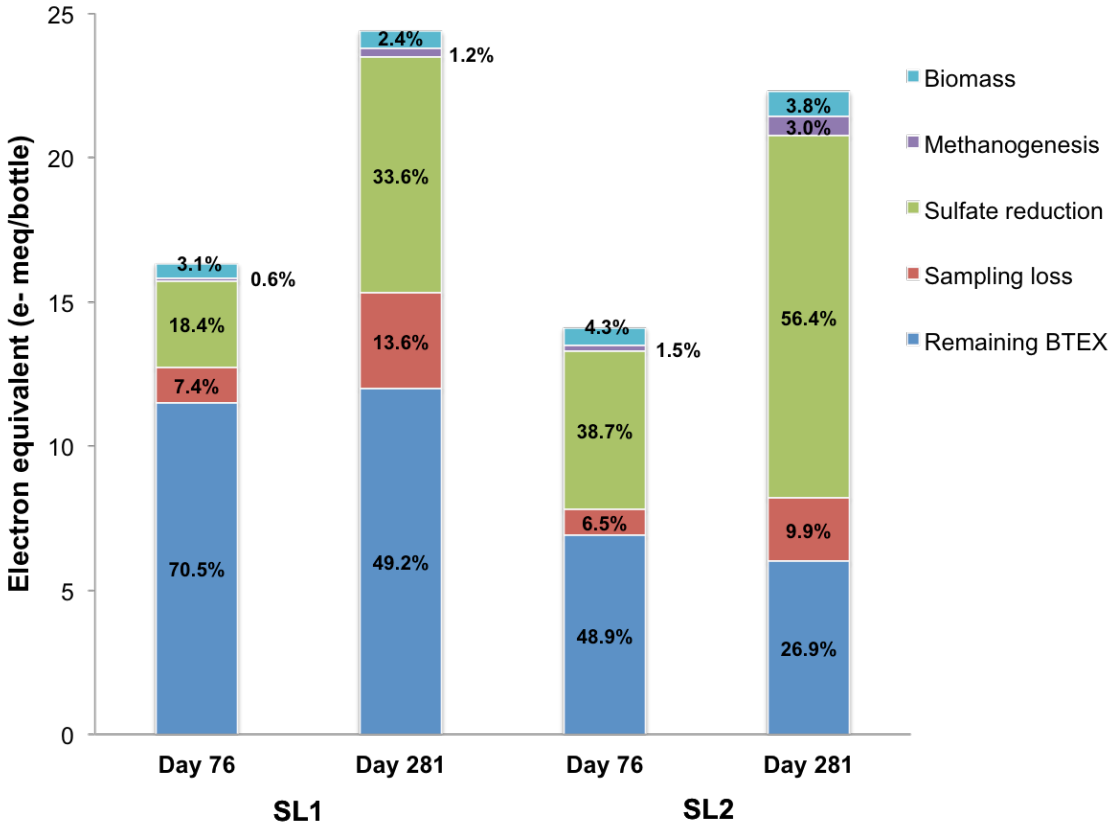

Figure 5. The electron-equivalent mass balances (1) on Day 76 with toluene completely biodegraded, but most benzene remained; (2) on Day 281 with re-spiked toluene completely removed. Sampling loss was calculated based on sampling volume and corresponding concentration in either gas phase or liquid phase. Electron equivalents accounted for biomass were calculated as the electron equivalent difference between the initial benzene plus toluene and the other four "electron sinks" shown above.

The electron-equivalent balance shown in Figure 5 reveals that the contribution of sulfate reduction towards benzene and toluene oxidations was dominant and consistent

over time: sulfate reduction accounted for 80% to 90% of the electrons released from benzene and toluene (assuming full oxidation) on Day 76 and Day 281 in each bottle. Methanogens consumed a small portion of electrons from toluene and benzene (<6%).

Although anaerobic benzene degradation linked to sulfate reduction has been reported, most of the reports were for petroleum-contaminated conditions in which the microbial communities had been stimulated by benzene or other aromatic compounds for a long period. Typically, obligately anaerobic biodegradation of toluene is considered to occur relatively more slowly (1.4 mmol/L biodegraded over 40 days in SL2) than aerobic biodegradation. Assuming a 5-meters biobarrier with groundwater flow rates from 0.003 to 3 m/d, the removal capacity for toluene is from 5000 to 5 mg/L, respectively, which is higher than most of the toluene concentrations in contaminated groundwater.

3.3 Conclusions

After 281 days of incubation, sulfate reduction was the dominant electron-accepting process when toluene was completely biodegraded in two batch experiments with benzene and toluene added as electron donors. The inoculum, from the anaerobic digester of a wastewater treatment plant, was able to biodegrade toluene coupled to sulfate reduction in the presence of benzene, even though benzene biodegradation was minimal. The culture started with the higher concentration of toluene had faster toluene biodegradation when challenged with re-spiked toluene, probably due to it having more capable biomass. Methanogenesis was a small electron sink during toluene biodegradation.

Although the biodegradation rate of toluene coupled to sulfate reduction basically meets the removal capacity requirement with typical flow rates and concentrations, it

does not support sulfate reduction as a promising method to stimulate groundwater bioremediation of toluene with benzene coexistence, due to the minimal biodegradation rate for benzene.

CHAPTER 4

AEROBIC BENZENE AND TOLUENE DEGRADATION WITH SUFFICIENT AND DEPLETED DISSOLVED OXYGEN

4.1 Experimental Setup

The reactors used in this study included closed batch reactors and a half-opened batch reactor with headspace connecting to a gas tank. In brief, the closed batch reactors were 240-mL serum bottles sealed with rubber stoppers and aluminum crimps. Each bottle had a liquid volume of 140 mL and a headspace volume of 100 mL. The half-open batch reactor was a 1-L medium bottle with 550-mL aqueous phase and 560-mL headspace. Figure 6 presents a schematic of the half-open batch reactor. The reactor was sealed by a rubber stopper and plastic cap, and its headspace was connected to a gas tank suppling 2% O_2, 5% CO_2, and the balance N_2. A liquid sampling port was set up by inserting a tubing into the aqueous phase through the stopper. A stirrer was set at the bottom to ensure a completely mixed aqueous phase.

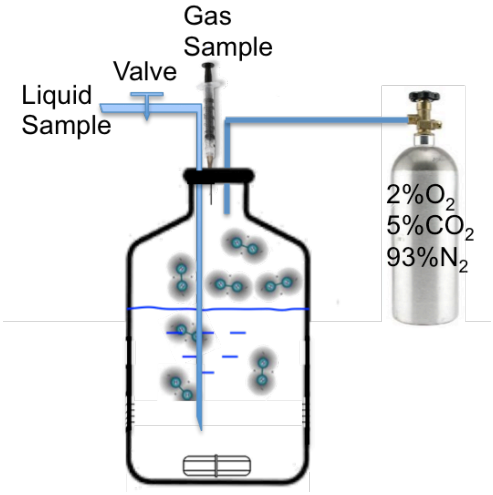

Figure 6. Schematic of the 1-L half-open batch reactor. The headspace was connected to a gas tank.

I used a modified Hunter's mineral base (MSB) as the carbon-free medium (Cohen-Bazire et al., 1957). It was composed of (mg/L): 3000 KH_2PO_4, 3110 Na_2HPO_4, 1000 $(NH_4)_2SO_4$, 50 $CaCl_2$-$2H_2O$, 300 $MgSO_4$-$7H_2O$, 7 $FeSO_4$-$7H_2O$, 3.1 EDTA, and 1 mL of trace mineral solution as described in Chapter 3. The carbon-free medium was prepared in a 1-L glass medium bottle and autoclaved before experiments. *Pseudomonas putida* strain F1 was obtained from the American Type Culture Collection (ATCC 700007). *P. putida* F1 was initially grown aerobically at 30°C in a broth medium containing beef extract (3 g/L) and peptone (5 g/L), and then it was transferred to another medium featuring benzene and toluene as electron donors, as well as carbon sources. Cultures grown on benzene were maintained at -80˚C in glycerol for future use.

The closed batch reactor was used for benzene and toluene degradation experiments having sufficient dissolved oxygen; therefore, the medium was air saturated. The half-open batch reactor was designed for benzene and toluene degradation experiments with depleted dissolved oxygen, and the medium was first aerated by water-vapor-saturated gas containing 2% O_2, 5% CO_2, and 93% N_2 to decrease the partial pressure of O_2 in the headspace to 2% and DO to around 0.6 mg/L.

Pure benzene and toluene were directly injected by gas-tight syringes into the serum bottles and medium bottle. The bioreactors were then stirred and maintained at 30°C for at least 24 hours to allow equilibrium of the benzene and toluene between the liquid and gas phase. Bacteria inoculated to these two experiments were *Pseudomonas putida* F1, which were pre-adapted to benzene and toluene to shorten the lag time.

Analyses carried out in this study included concentrations of suspended biomass (measured as optical density), benzene and toluene concentration in gas and liquid,

intermediates concentrations in the liquid, and the dissolved oxygen concentration. Details of the analytical methods are described in Chapter 2.

4.2 Results and Discussion

4.2.1 Stoichiometry and Kinetic Model

Hydroxylation and dehydrogenation reactions correspond to conventional mineralization reactions that do not take oxygenation reactions into account. For this case, the standard half reactions (R_d) for the electron donors, benzene and toluene, are written as a reduction from H_2CO_3 for one electron equivalent:

$$\text{Benzene: } \frac{6}{30}H_2CO_3 + H^+ + e^- = \frac{1}{30}C_6H_6 + \frac{18}{30}H_2O \qquad (18)$$

$$\Delta G_d^{0'} = 26.53\ kJ / e^- eq$$

$$\text{Toluene: } \frac{7}{36}H_2CO_3 + H^+ + e^- = \frac{1}{36}C_7H_8 + \frac{21}{36}H_2O \qquad (19)$$

$$\Delta G_d^{0'} = 26.43\ kJ / e^- eq$$

These two reactions indicate that full mineralization of one mole of benzene and toluene yield 30 and 36 electron equivalents, respectively. However, as described in Chapter 2, oxygenation activation reactions do not yield net release of electrons to the electron acceptor to generate energy; therefore, they significantly alter the energy and electron balance for the microbial utilization of benzene and toluene. Figure 6 shows the degradation pathway. Tables 1 and 2 summarize all the electron donor reactions for each step of benzene and toluene degradation via dioxygenase pathways.

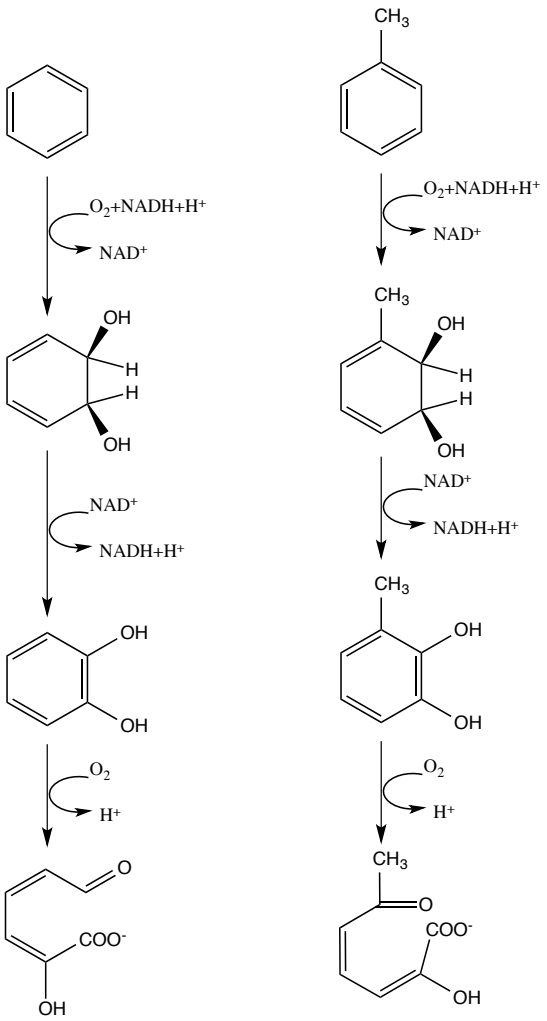

Figure 7. Biodegradation pathway of benzene and toluene via the dioxygenase pathways. The pathways yield no net production of $NADH+H^+$, and O_2 is a direct reactant.

Table 1. Electron donor reactions and electron flows for each step of benzene degradation

Rxn.		*H*	*R*	*T*	*O*
1. Dioxygenation step one	$C_6H_6+O_2+2H^++2e^-=C_6H_8O_2$	28	2	-2	4
2. Dehydrogenation (step two)	$C_6H_8O_2=C_6H_6O_2+2H^++2e^-$	26	2	2	0
3. Dioxygenation	$C_6H_6O_2+O_2=C_6H_5O_4^-+H^+$	22	4	0	4
4. Multiple hydroxylations and dehydrogenations	$C_6H_5O_4^-+14H_2O=6H_2CO_3+21H^++22e^-$	0	22	22	0
One step reaction	$C_6H_6+14H_2O+2O_2=6H_2CO_3+22H^++22e^-$	0	30	22	8

Table 2. Electron donor reactions and electron flows for each step of toluene degradation

Rxn.		*H*	*R*	*T*	*O*
1. Dioxygenation step one	$C_7H_8+O_2+2H^++2e^-=C_7H_{10}O_2$	34	2	-2	4
2. Dehydrogenation (step two)	$C_7H_{10}O_2=C_7H_8O_2+2H^++2e^-$	32	2	2	0
3. Dioxygenation	$C_7H_8O_2+O_2=C_7H_7O_4^-+H^+$	28	4	0	4
4. Multiple hydroxylations and dehydrogenations	$C_7H_7O_4^-+17H_2O=7H_2CO_3+27H^++28e^-$	0	28	28	0
One step reaction	$C_7H_8+17H_2O+2O_2=7H_2CO_3+28H^++28e^-$	0	36	26	8

For the case of the oxygenation activation, complete mineralization of one mole benzene and toluene directly incorporates two moles of O_2 for activation, and the standard reduction half reactions (R_d) that include O_2 are:

$$\text{Benzene: } \frac{6}{22}H_2CO_3 + H^+ + e^- = \frac{1}{22}C_6H_6 + \frac{14}{22}H_2O + \frac{2}{22}O_2(g) \quad (20)$$

$$\Delta G_d^{0'} = 64.74 \ kJ / e^- eq$$

$$\text{Toluene: } \frac{7}{28}H_2CO_3 + H^+ + e^- = \frac{1}{28}C_7H_8 + \frac{17}{28}H_2O + \frac{2}{28}O_2(g) \quad (21)$$

$$\Delta G_d^{0'} = 56.42 \ kJ / e^- eq$$

These two reactions indicate that only 22 and 28 electron equivalents per mole of benzene and toluene, respectively, are available for energy generation or biomass synthesis, and other electron equivalents are invested to reduce oxygen molecules.

The half reaction (R_a) for the utilization of molecular oxygen as the electron acceptor is:

$$\frac{1}{4}O_2(g) + H^+ + e^- = \frac{1}{2}H_2O \quad (22)$$

$$\Delta G_a^{0'} = -78.06 \ kJ / e^- eq$$

Table 3 summarizes all the key parameters for the estimation of the overall stoichiometry for mineralization of benzene using Equations (2), (6), (7), (9), and (10). Pyruvate is assumed to be a carbon source for bacteria, making $\Delta G_c^{0'} = 35.09 kJ / e^- eq$.

Table 3. Key parameters and calculated values for mineralization of benzene and toluene

	Benzene	**Toluene**
$\Delta G_d^{0'}$	64.74 kJ/e^-eq	56.42 kJ/e^-eq
$\Delta G_a^{0'}$	-78.06 kJ/e^-eq	
$\Delta G_r^{0'}$	-142.8 kJ/e^-eq	-134.48 kJ/e^-eq
$\Delta G_p^{0'}$	35.09 kJ/e^-eq	
$\Delta G_c^{0'}$	35.09 kJ/e^-eq	
$\Delta G_{pc}^{0'}$	18.8 kJ/e^-eq	
$\Delta G_{syn}^{0'}$	31.33 kJ/e^-eq	
T	22/30 = 0.733	28/36 = 0.778
O	8/30 = 0.267	8/36 = 0.212
A	0.366	0.388
f_s^0	0.537	0.560
f_e^0	0.196	0.218
n	+1	
ε	0.6	

Substituting T, f_s^0, and f_e^0 values into Equation (11) leads to the following overall stoichiometry for benzene and toluene, respectively:

$$\begin{aligned} &C_6H_6 + 0.808\,NH_4^+ + 3.483O_2(g) + 0.571H_2O \\ &= 0.811H^+ + 1.982\,H_2CO_3 + 0.808\,C_5H_7O_2N \end{aligned} \tag{23}$$

$$\begin{aligned} &C_7H_8 + 1.008\,NH_4^+ + 3.962\,O_2(g) \\ &= H^+ + 1.96\,H_2CO_3 + 1.008\,C_5H_7O_2N + 0.028\,H_2O \end{aligned} \tag{24}$$

4.2.2 Aerobic Benzene and Toluene Degradation with Sufficient DO

The initial benzene and toluene concentrations were different in the two batch tests due to small injection volumes, which led to deviations from the target concentrations. The initial DO in this closed system was 8 mg/L. As DO was consumed by aerobic biodegradation, oxygen in the headspace re-partitioned to the aqueous phase. The initial concentration of the electron-donor substrate was set on the basis of stoichiometry (Equations 23 and 24) to ensure a DO level higher than 2.5 mg/L after complete benzene and toluene mineralization and partitioning of O_2 from the gas phase. 1 mL of *P. putida* F1 inoculum was provided to each reactor from the pre-adapted culture, which led to an initial biomass concentration of 2 mgVSS/L.

Figure 7 presents the optical densities and the mass concentrations of benzene and toluene in two closed batch experiments. During the first 4 hours, concentrations of benzene and toluene gradually decreased, while the biomass concentration, corresponding to the optical density, showed little increase. This may indicate an initial partitioning of the volatile substrates to the gas phase. Or, it may have been caused by a "lag" time needed to have dioxygenation intermediates produced and then oxidized by hydroxylation and dehydrogenation reactions.

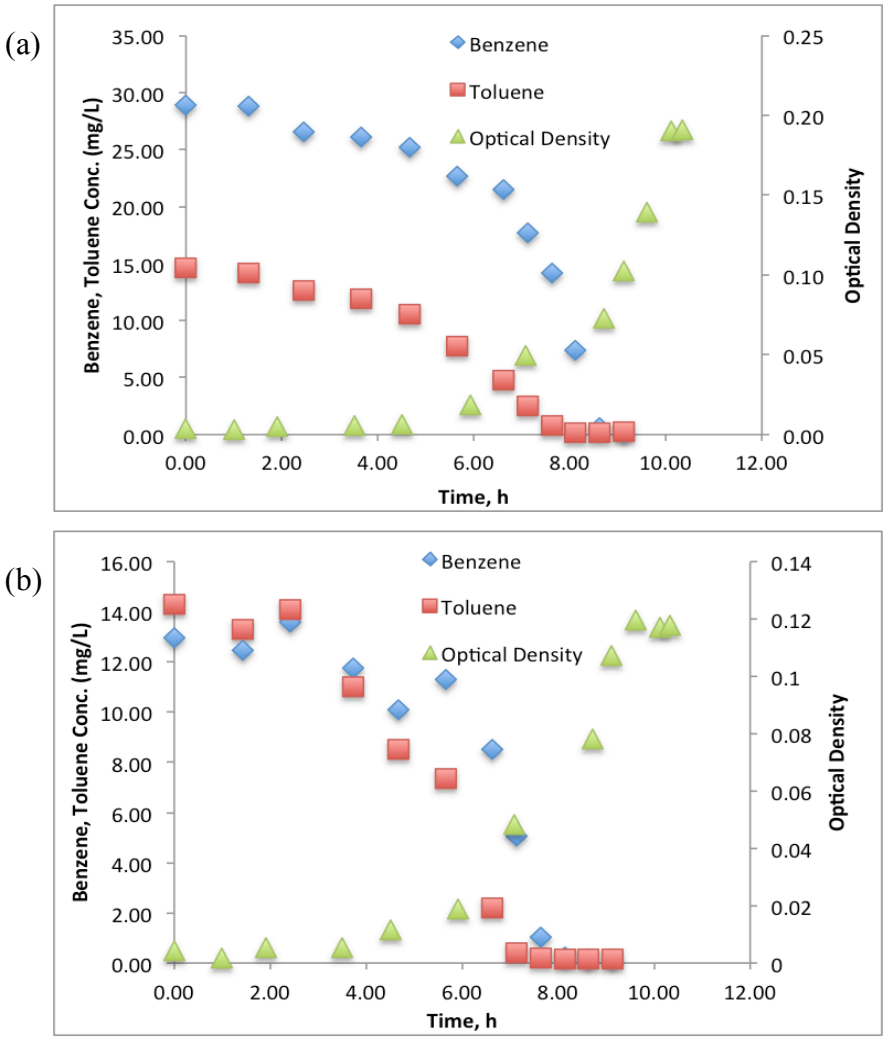

Figure 8. Mass concentration of benzene and toluene, and optical density in the two inoculated serum bottles.

After nine hours (Fig. 7a) or eight hours (Fig. 7b), almost all of the benzene and toluene was consumed. The biomass concentration showed substantial increase after 6 hours, and it kept increasing even after benzene and toluene were completely removed. This trend supports that the accumulation and subsequent oxidation of intermediates controlled bacterial growth (Chang et al., 1993). The stoichiometry in Tables 1 and 2 show that initial di-oxygenations of benzene and toluene do not yield a net release of electrons to support energy generation and biomass synthesis.

4.2.3 Aerobic Benzene and Toluene Degradation with Depleted DO

In this experiment, after the medium was sparged by water-vapor-saturated 2% O_2 gas, the initial DO was 0.6 mg/L. The initial concentrations of benzene and toluene were 28.2 and 11.1 mg/L, respectively. I inoculated the reactor with 10 mL of *P. putida* F1 inoculum from the pre-adapted stock culture, leading to an initial biomass concentration of 8.5 mgVSS/L.

Figure 8 presents the DO, total molar masses of benzene, catechol, toluene, 3-methylcatechol, and VSS computed from OD values in this depleted-DO experiment. In the previous batch experiments with high DO, I did not measure the di-oxygenated intermediates, but I measured them in this experiment. During the first 30 hours, catechol gradually accumulated along with the benzene concentration decreasing, while 3-methycatechol showed only a small accumulation at the beginning and then gradually decreased, despite rapid toluene removal. Benzene and toluene degradation, as well as catechol accumulation, stopped almost at the same time after 30 hours.

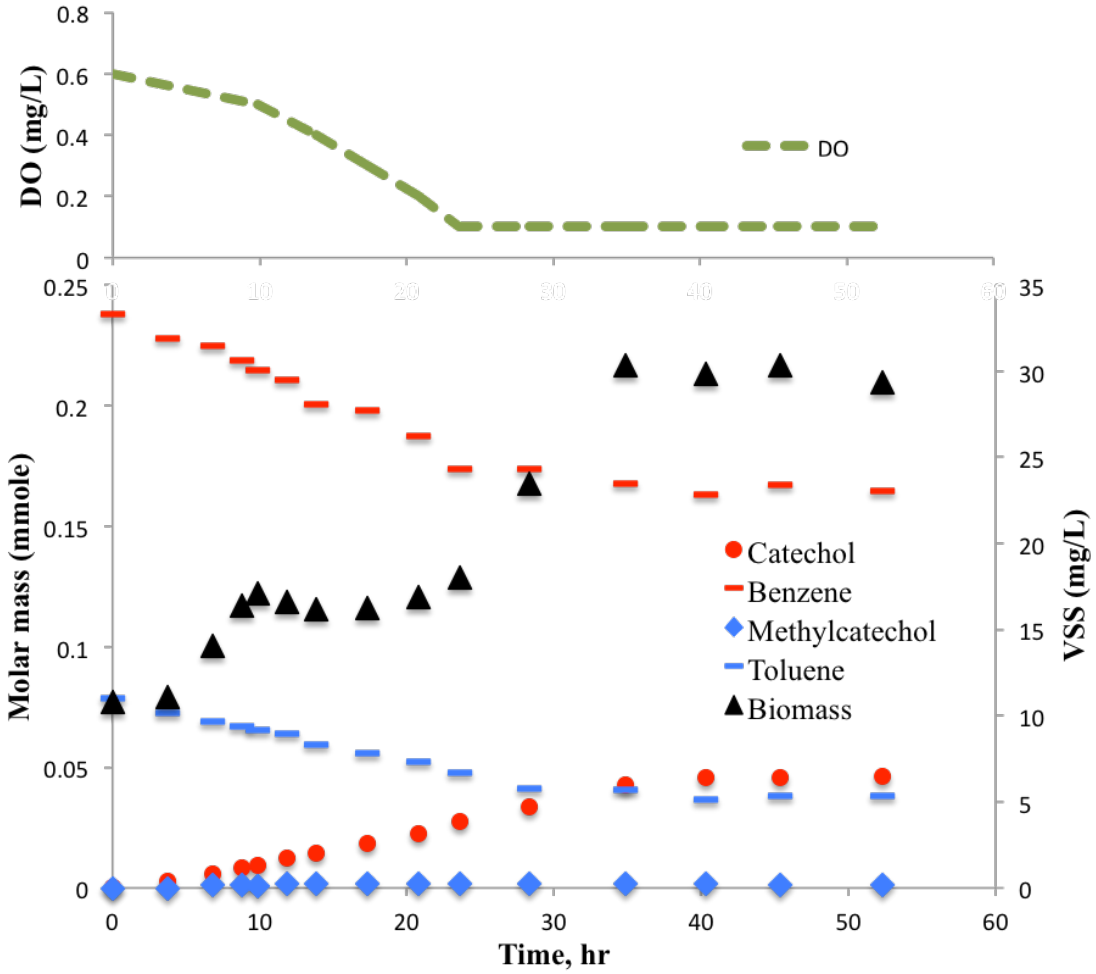

Figure 9. Total molar mass of benzene, catechol, toluene, 3-methylcatechol, VSS (bottom), and DO (top) along with time in the 1-L half-opened batch reactor. The values of mgVSS/L were computed from OD values.

Sampling loss was calculated based on sampling volume and corresponding concentration in either gas phase or liquid phase. Excluding sampling loss, the total benzene loss was 0.057 mmole and total catechol production is 0.046 mmole; so, over 80% of the consumed benzene was transformed to catechol and did not support biomass growth during the experiment. The total removed toluene was 0.039 mmole, and 3-methylcatechol residual was 0.001 mmole. Although an undefined peak on the chromatograms could have be another intermediate (probably 4-methylcatechol), its peak areas were always much smaller than 3-methylcatechol. Thus, most of the toluene

removed from the system could be fully oxidized and supported biomass synthesis. Since only oxidation of the intermediates could support bacterial growth, a significant biomass increase during this period was mainly contributed by toluene mineralization.

After 30 hours, no further biodegradation occurred. The cessation of biodegradation processes probably was due to depletion of the limited DO, which had fallen below 0.1 mg/L after 30 hours (Figure 8). This reactor was originally designed to keep a constant partial pressure of oxygen in the headspace, thereby giving a constant low concentration of DO. However, the supply of gas containing only 2% O_2 from the gas tank was not sufficient to maintain a DO concentration of 0.6 mg/L.

Inconsistent with the cessation of degradation processes, the experimental data shows that biomass was still increasing after 30 hours. Relationship between biomass growth and substrate utilization should be explored to better explain the inconsistence. Following the method of Yu et al. (2001b), discussed in Chapter 2, Equation (25) and Equation (26) give the mass balance for the original substrates (S_1, benzene or toluene) and one di-oxygenation intermediate (S_2, catechol or 3-methylcatechol, assuming the second di-oxygenation is fast), respectively.

$$\frac{dS_1}{dt} = -\left[\frac{q_{1,\max} S_1}{K_1 + S_1}\right]\left[\frac{S_O}{K_O + S_O}\right]\left[\frac{S_{NAD(H)}}{K_{NAD(H)} + S_{NAD(H)}}\right] X_a \cdot \frac{V_l}{V_l + V_g H} \tag{25}$$

$$\frac{dS_2}{dt} = \underbrace{\alpha_{12}\left[\frac{q_{1,\max} S_1}{K_1 + S_1}\right]\left[\frac{S_O}{K_O + S_O}\right]\left[\frac{S_{NAD(H)}}{K_{NAD(H)} + S_{NAD(H)}}\right] X_a}_{Term1} - \underbrace{\left[\frac{q_{2,\max} S_2}{K_2 + S_2}\right]\left[\frac{S_O}{K_O + S_O}\right] X_a}_{Term2} \tag{26}$$

Equation (26) shows that the intermediate is produced from activation of the original substrate (Term 1) and utilized by subsequent hydroxylation and dehydrogenation

reactions (Term 2). In these two equations, α_{12} is the stoichiometric coefficient for the production of the intermediates from primary substrate. Subscript 1, 2, O, and NAD(H) refer to variables for original substrate, intermediate, dissolved oxygen, and intracellular electron carrier, respectively. As described in Chapter 2, a correction term was added at the end of Equation (25); it converts total mass to the mass in liquid phase. However, no such term is in Equation (26), because intermediates are assumed to present only in liquid phase due to their relatively low Henry's constant.

Equations (27) to (29) describes the non-steady-state mass balance for biomass, where X_i is the inert biomass concentration, X_v is the volatile suspended solids concentration, Y is the biomass true yield for the intermediates utilization, *b* is the decay coefficient, and f_d is the biodegradable active biomass (Rittmann & McCarty, 2001):

$$\frac{dX_a}{dt} = Y\underbrace{\left[\frac{q_{2,\max}S_2}{K_2+S_2}\right]\left[\frac{S_O}{K_{O,2}+S_O}\right]X_a}_{Term1} - b\cdot X_a \tag{27}$$

$$\frac{dX_i}{dt} = (1-f_d)\cdot b\cdot X_a \tag{28}$$

$$\frac{dX_v}{dt} = \frac{d(X_a+X_i)}{dt} = Y\left[\frac{q_{2,\max}S_2}{K_2+S_2}\right]\left[\frac{S_O}{K_{O,2}+S_O}\right]X_a - f_d\cdot b\cdot X_a \tag{29}$$

According to previous theoretical and experimental results, I assumed only intermediates utilization – Term 1 in Equation (27), which is proportional to Term 2 in Equation (26) – supports synthesis of active biomass.

To link biomass growth directly to S_1 and S_2 utilization, substituting Equation (25) into Equation (26) gives Equation (30), and then substituting Equation (30) into Equation

(29) leads to Equations (31).

$$\frac{dS_2}{dt} = -\alpha_{12}\frac{V_l + V_g H}{V_l}\cdot\frac{dS_1}{dt} - \left[\frac{q_{2,\max}S_2}{K_2 + S_2}\right]\left[\frac{S_0}{K_0 + S_0}\right]X_a \tag{30}$$

$$\frac{dX_v}{dt} = Y\left(-\alpha_{12}\frac{V_l + V_g H}{V_l}\cdot\frac{dS_1}{dt} - \frac{dS_2}{dt}\right) - f_d b X_a \tag{31}$$

Equation (31) describes the relationship between biomass growth, original and intermediate substrate utilization, as well as active biomass concentration. From the stoichiometry developed previously, α_{12} equals 1.41 g-S_2/g-S_1 and 1.35 g-S_2/g-S_1 for benzene and toluene, and Y equals 0.83 g-X_a/g-S_2 and 0.92 g-X_a/g-S_2 for benzene and toluene, respectively. The fraction of the active biomass that is biodegradable (f_d) is set to 0.8, and the decay coefficient b equals 0.06 d^{-1} according to (Yu et al., 2001b). In this model, the input values were experimental data from benzene, toluene (S_1), and their dioxygenation intermediates catechol and 3-methylcatechol (S_2); the output values were biomass concentrations (X_v).

Figure 9 compares experimental and modeled data for biomass growth on benzene and toluene in this experiment. The modeled biomass growth curve was not smooth, because the input values were experimental data. The modeled results are almost identical to the experimental results during the first 25 hours, indicating the assumption of the two-step model was basically correct: Only the oxidation of di-oxygenation intermediates caused bacterial growth. However, the experimental results increased dramatically after 25 h, while the model results stabilized and gradually declined. The measured biomass results are not consistent with other experimental data: Despite no substrate utilization after 30 hours, the measured biomass concentration was still

increasing. The likely reason for the difference between experimental and modeled data is that the culture medium changed color during the biodegradation of benzene, and this could have led to overestimating biomass by OD (Reardon et al., 2000). Thus, filtered samples rather than initial medium should have been used as optical density blanks for every sample's optical density measurement, or, VSS should have been measured directly.

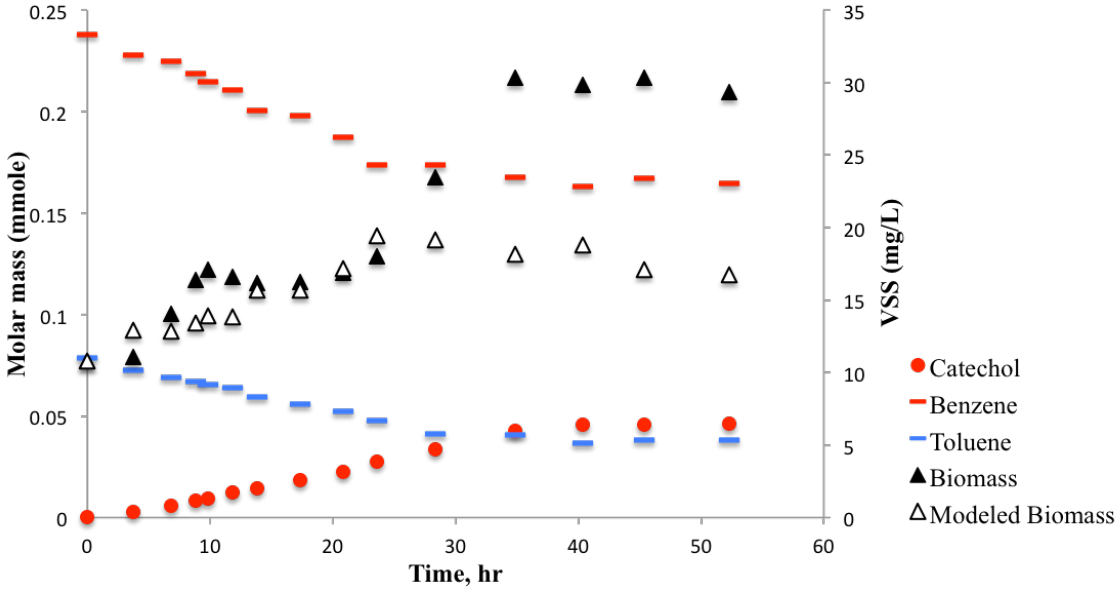

Figure 10. Comparison of experimental and modeled data for biomass growth on benzene and toluene. The experimental values of mgVSS/L were computed from OD values.

4.3 Conclusions

Oxygenation reactions alter electron and energy balances for benzene and toluene mineralization. Full mineralization of 1 mole benzene and 1 mole toluene with normal hydroxylation and dehydrogenation reactions yields 30 and 36 electron equivalents for respiration and biomass synthesis, respectively. Adding the initial di-oxygenation steps lowers the net yield of electron to respiration and energy generation to 22 and 28 per mole, respectively. Thus, adding di-oxygenation reactions as activation steps lowers the overall yield for full mineralization, and it also may delay synthesis if intermediates

accumulate.

In the fully aerobic biodegradation experiments, benzene and toluene were utilized by *P. putida* F1 with a lag in biomass production and continued biomass growth after complete substrate removal. The lag occurs because energy generation to support biomass synthesis was tied to oxidation of di-oxygenation intermediates, rather than directly to benzene and toluene transformation.

In the half-open batch experiment, the di-oxygenation intermediate, catechol, accumulated during benzene's aerobic degradation with limited DO, but this condition was practically difficult to maintain in this experiment. Considering 80% of removed benzene converted to catechol without further oxidation, the removed toluene without intermediates accumulation was completely mineralized to generate electrons and energy for biomass growth. Modeled biomass growth fit the experimental results well during the first half of the experiment, which once again supported the explanation that oxidation of di-oxygenation intermediates caused biomass growth. However, modeled biomass growth deviated from the experimental results during the second half period due to medium color.

CHAPTER 5

ANAEROBIC CATECHOL DEGRADATION COUPLED TO SULFATE OR NITRATE REDUCTION

5.1 Experimental Setup

As observed in Chapter 4, catechol could accumulate as an intermediate from benzene aerobic degradation with depleted oxygen. I designed experiments to test if sulfate- or nitrate-reducing bacteria were able to utilize catechol anaerobically to allow benzene mineralization if catechol were formed. The reactors used in this study included closed batch reactors and a 1-D column reactor used to evaluate biostimulation. The main goal of biostimulation was to activate endogenous sulfate- or nitrate-reducing bacteria capable of catechol biodegradation from different inocula sources, such as wastewater treatment plant and petroleum-contaminated soil or sediment sites.

I used the same carbon-free medium as described in Chapter 3, which was composed of (in g/L) 0.1 $MgCl_2$, 0.1 $CaCl_2$, 1 NH_4Cl, 1 K_2HPO_4, 2 Na_2SO_4, and 1 mL of trace mineral solution. Similar to the reactors described in Chapter 4, the closed batch reactors were 240-mL serum bottles sealed with rubber stoppers and aluminum crimps; they had a 140-mL liquid volume, leaving a 100-mL headspace. The inocula for these experiments were anoxic sludge from Mesa Northwest Water Reclamation Plant. Before each experiment, I incubated the sludge with pyruvate as the sole electron donor and sulfate or nitrate as the electron acceptor to enrich sulfate- or nitrate-reducing bacteria. I also added 50 mM 2-bromoethane sulfonic acid (BES) into each reactor to eliminate methanogens (Parameswaran et al., 2009). After enrichment (indicated by the complete consumption of sulfate or nitrate), I transferred centrifuged sludge to new bottles for biostimulation

tests with catechol.

The 1-D reactor was a 1.5-L column with five sampling ports on the side and recirculation tubing connecting the top and bottom of the column. Figure 10 presents a schematic of the column reactor used for biostimulation. This biostimulation column (BSC) was operated as an up-flow anaerobic sludge blanket (UASB) reactor in a sequencing batch mode.

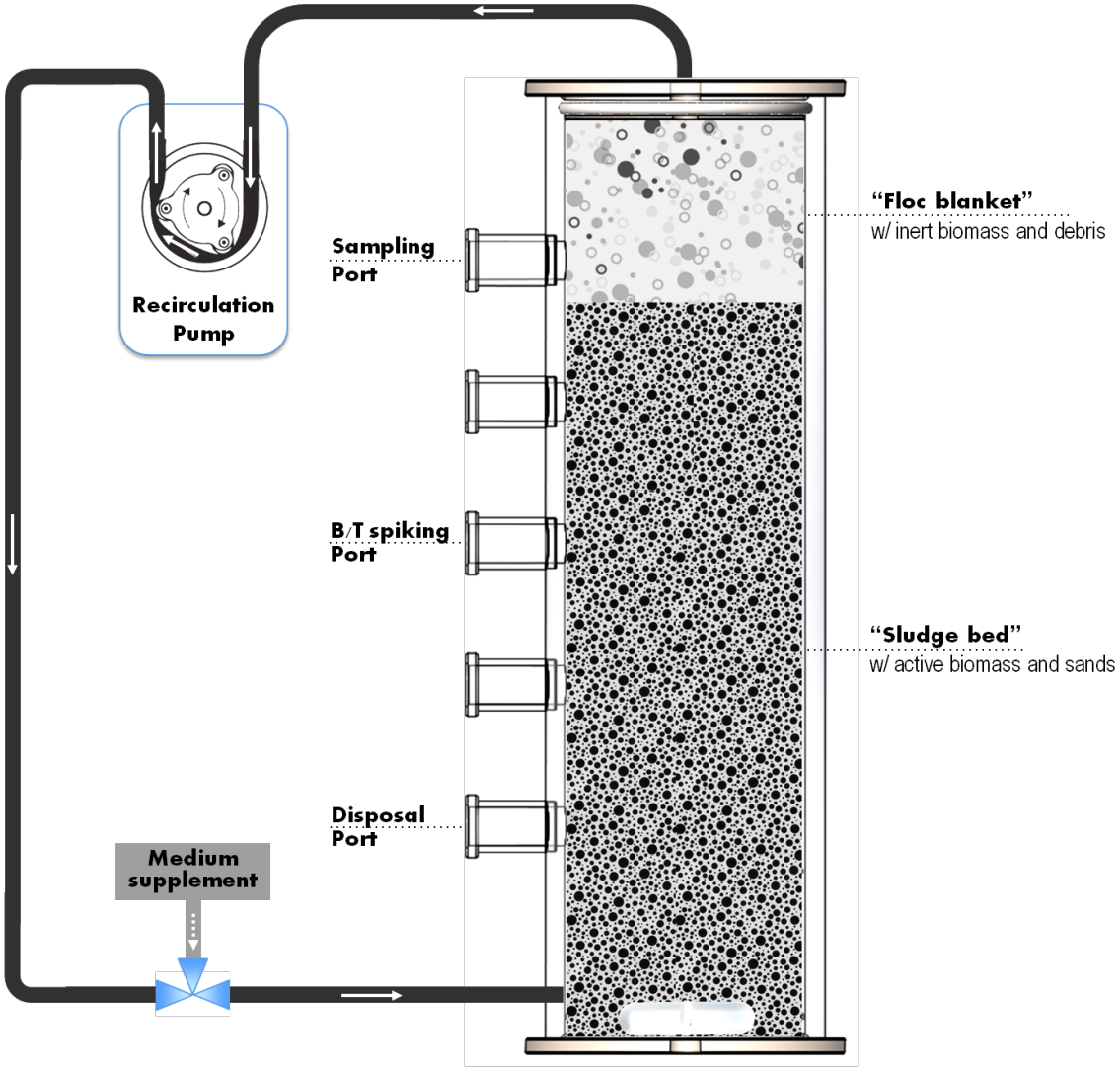

Figure 11. Schematic of the biostimulation column (BSC).

The BSC was one-quarter packed with soils from heavily petroleum-contaminated

sites. Inocula from contaminated soils may be better adapted to biodegrading benzene and toluene, as well as biodegradation intermediates such as catechol. I screened the soils in advance, leaving only granular sands and sludge. Then, the BSC was placed in the anaerobic glove box and filled with anaerobic, carbon-free nutrient medium, as well as 1 mL trace metals solution and 10 mL ATCC multi-vitamin supplement, including (mg/L): 2.0 Folic acid, 10.0 Pyridoxine hydrochloride, 5.0 Riboflavin, 2.0 Biotin, 5.0 Thiamine, 5.0 Nicotinic acid, 5.0 Calcium Pantothenate, 0.1 Vitamin B12, 5.0 p-Aminobenzoic acid, 5.0 Thioctic acid, and 900.0 Monopotassium phosphate. A magnetic stir bar at the bottom was rotated at a moderate speed (~ 300 rpm) to ensure uniform influent distribution and avoid formation of firm settled layer at the bottom. Within 15 minutes, two distinguishable zones formed in the column: the lower "sludge bed" zone of rapid settling sands and biomass sludge, and the upper "floc blanket" zone of poorly settleable flocs. After the formation of the zones, the BSC was sealed and taken out from the anaerobic glove box; then it was operated in the batch mode with up-flow recirculation using a peristaltic pump. With a suitable recirculation flow velocity, the heavier "bed" zone gradually swelled upwards to third-quarter of the column depth and stayed at this stable height. The upper solid/liquid mixture in the "floc blanket" zone moved upward, steadily leaving from the port at the top of the column and recirculating to the bottom. This zoning strategy prevented the large sand aggregates in the "bed" zone from clogging the recirculation tubing and the sampling needles. With recirculation stabilized, concentrated sulfate and nitrate from stock solutions were injected into the BSC through the third sampling port. The system was initially spiked with 150-μM catechol from concentrated stock solution as the sole exogenous electron donor, although

the inocula contained endogenous organics. 4 mM $NaHCO_3$ was added to the system as a cosubstrate (Ding et al., 2008; Milligan & Häggblom, 1998). Because of the N_2 gas production from denitrification, gas was occasionally collected from top of the column into a gas-tight Tedlar bag to prevent the reactor from overpressurizing. At the beginning and end of the experiment, I took bacterial samples from suspended sludge following the method described in Chapter 2.

Analyses carried out in this study included concentrations of nitrate, sulfate, nitrite, catechol, and soluble chemical oxygen demand (sCOD). Details of the analytical methods were described in Chapter 2.

5.2 Results and Discussion

5.2.1 Batch Study on Catechol Anaerobic Degradation Coupled to Sulfate or Nitrate Reduction

Figure 11 shows the results for SRB adaptation with pyruvate as the electron donor and sulfate as the electron acceptor. In stage 1, over 50% sulfate was consumed within 4 days; the results were similar in these two parallel batch reactors (labeled #1 and #2). In stage 2, sludge from #1 and #2 was centrifuged and transferred to another bottle (labeled #3) with higher concentration of sulfate and pyruvate than in stage 1. During stage 2, the sulfate concentration decreased by 84% in five days, indicating strong SRB activity.

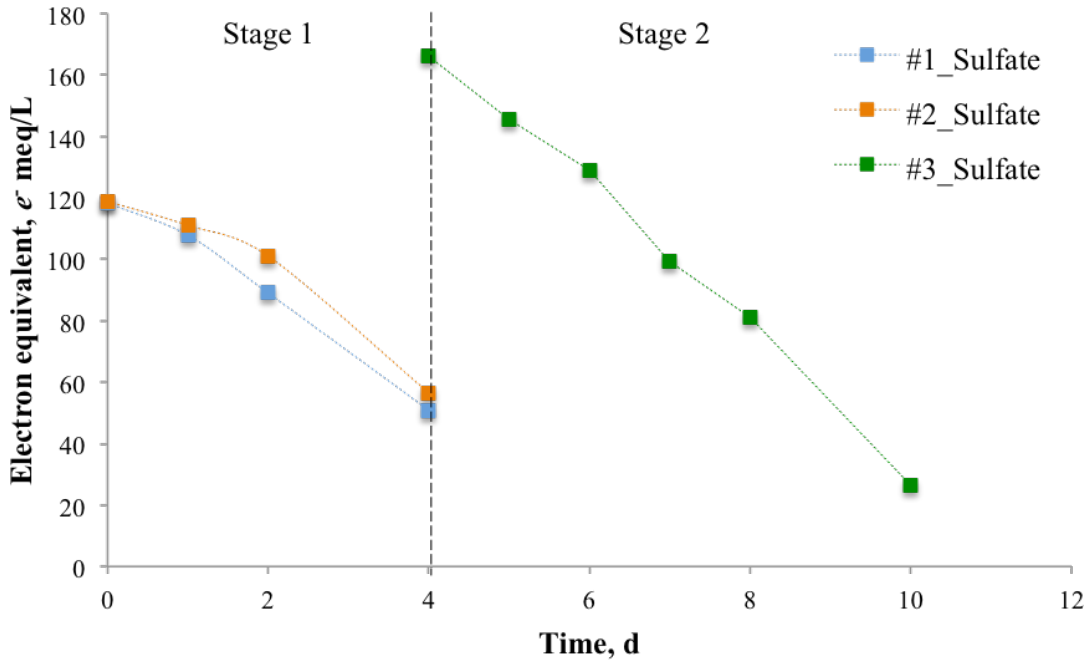

Figure 12. Results for SRB adaptation with pyruvate as the electron donor. #1, #2, and #3 indicates three batch reactors. Stage 1 and 2 indicates two adaptation experiments with different substrate concentrations. Concentrations were transformed to electron equivalents as described in Chapter 2.

Figure 12 shows the results for catechol biodegradation coupled to sulfate reduction. In stage 1, centrifuged sludge from previous SRB adaptation experiment was inoculated into two serum bottles (labeled as #1 and #2) with catechol as the sole exogenous electron donor and sulfate as the sole electron acceptor. Sulfate reduction was slower with catechol than with pyruvate, and its utilization rate decreased with time. From Day 3 to Day 9, catechol decreased by 11% in #2, while it remained stable in #1, and it did not show further decrease after Day 9 in either #1 or #2. The difference between catechol consumption in #1 and #2 also corresponded to the difference between sulfate decrease in these two bottles. In each bottle, the consumed catechol electron equivalents were less than those used for sulfate reduction. This difference suggests oxidation of endogenous electron donors, such as organic materials brought in with the inoculum; an alternate

explanation is that some electrons were trapped in forms of sulfur less reduced forms than sulfide, such as elemental sulfur (S°).

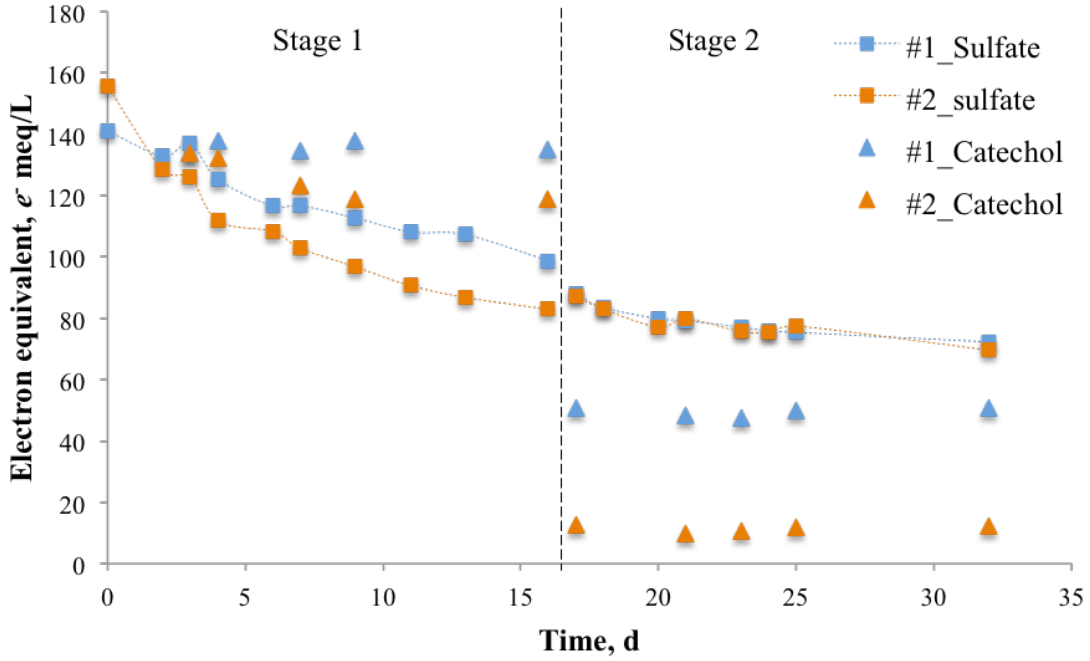

Figure 13. Results for catechol biodegradation coupled to sulfate reduction. #1 and #2 indicates two batch reactors. Stage 1 and 2 indicates two experiments with different initial substrate concentrations. Concentrations were transformed to electron equivalents as described in Chapter 2.

To minimize potential inhibition of cell synthesis by catechol in stage 2, I transferred the sludge from stage 1 into the same medium, but with lower concentrations of catechol and sulfate. The results were a slight sulfate decrease, but no catechol removal, indicating that the bacteria were not utilizing catechol as an electron donor to reduce sulfate.

Biodegradation of catechol is slow under anoxic conditions, and under sulfate-reducing condition it has been only studied with *Desulfobacterium* sp. strain Cat2, which formed protocatechuyl-coenzyme A (CoA) from catechol, bicarbonate, and uncombined CoA (Gorny & Schink, 1994). Thus, I also did biostimulation experiments of catechol

degradation with nitrate and sulfate as electron acceptors together. Similar to the experiments with only sulfate, the bacteria were first grown anaerobically on pyruvate with sulfate and nitrate as electron acceptors together. Then, I transferred adapted bacteria to three new bottles, two of which are parallel experiments with catechol as the sole electron donor, and the other one is a control without addition of catechol.

As shown in Figure 13, catechol decreased by 20% during the first day, but further degradation halted once nitrite began to accumulate. However, compared to the stable catechol concentration, nitrate gradually decreased even in the control group, which again infers the presence of endogenous electron donors responsible for denitrification, such as organic substances and possibly H_2S/S^0 (corresponding to 25% sulfate increasing) transferred from last stage.

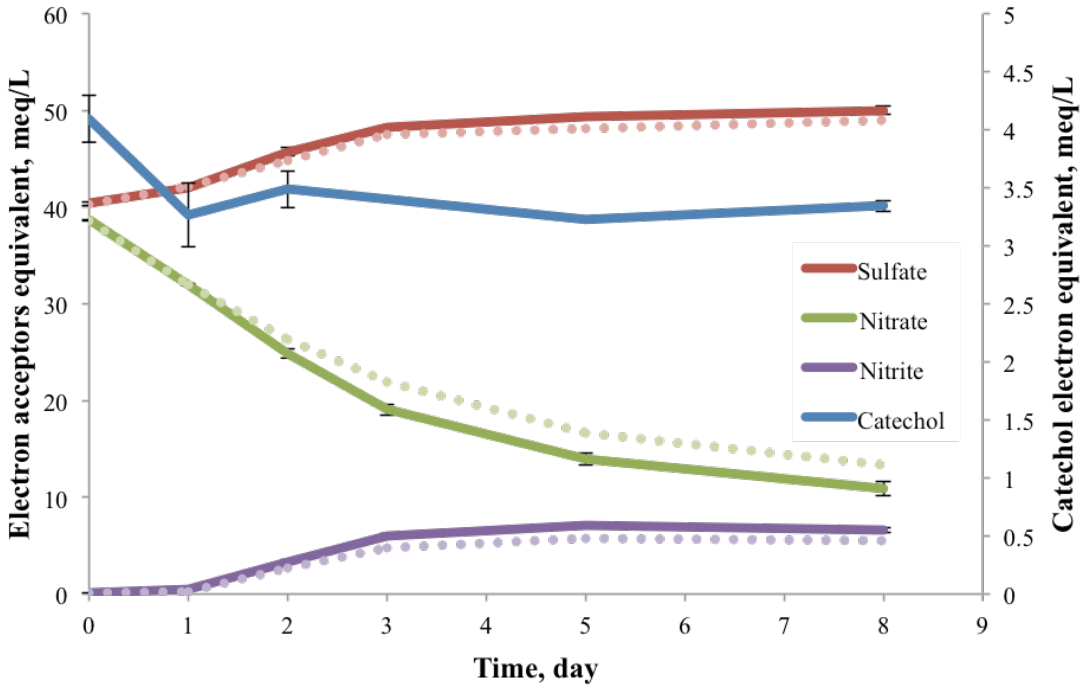

Figure 14. Results for catechol biodegradation coupled to nitrate and sulfate reductions. Dashed lines indicate the results from the control with no catechol. Units of substrate concentrations were transformed to electron equivalents as described in Chapter 2.

Nitrite accumulation, due to insufficient electron donor for complete denitrification, probably inhibited further catechol degradation by forming yellowish nitrite-catechol complexes (Ding et al., 2008; Milligan & Häggblom, 1998). Additional blank experiments proved that this yellowish product was not formed abiotically (Figure 14).

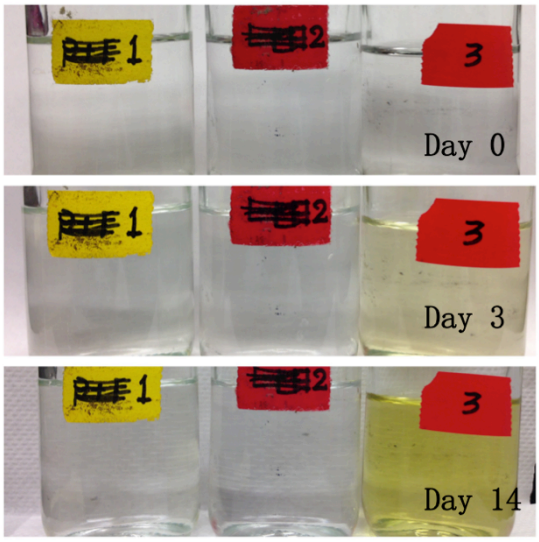

Figure 15. Formation of the yellowish nitrite-catechol product: #1 only catechol, #2 only nitrite, #3 catechol+nitrite.

5.2.2 Biostimulation Column Study on Catechol Anaerobic Degradation

As shown in Figure 15**,** nitrate was consumed very quickly due to the large amount of organic material (corresponding to sCOD values) brought into the system with sediment slurry or soil, along with denitrifiers being abundant in the inoculum. I periodically re-spiked NO_3^- to its initial concentration (100 mgN/L) when it was completely removed.

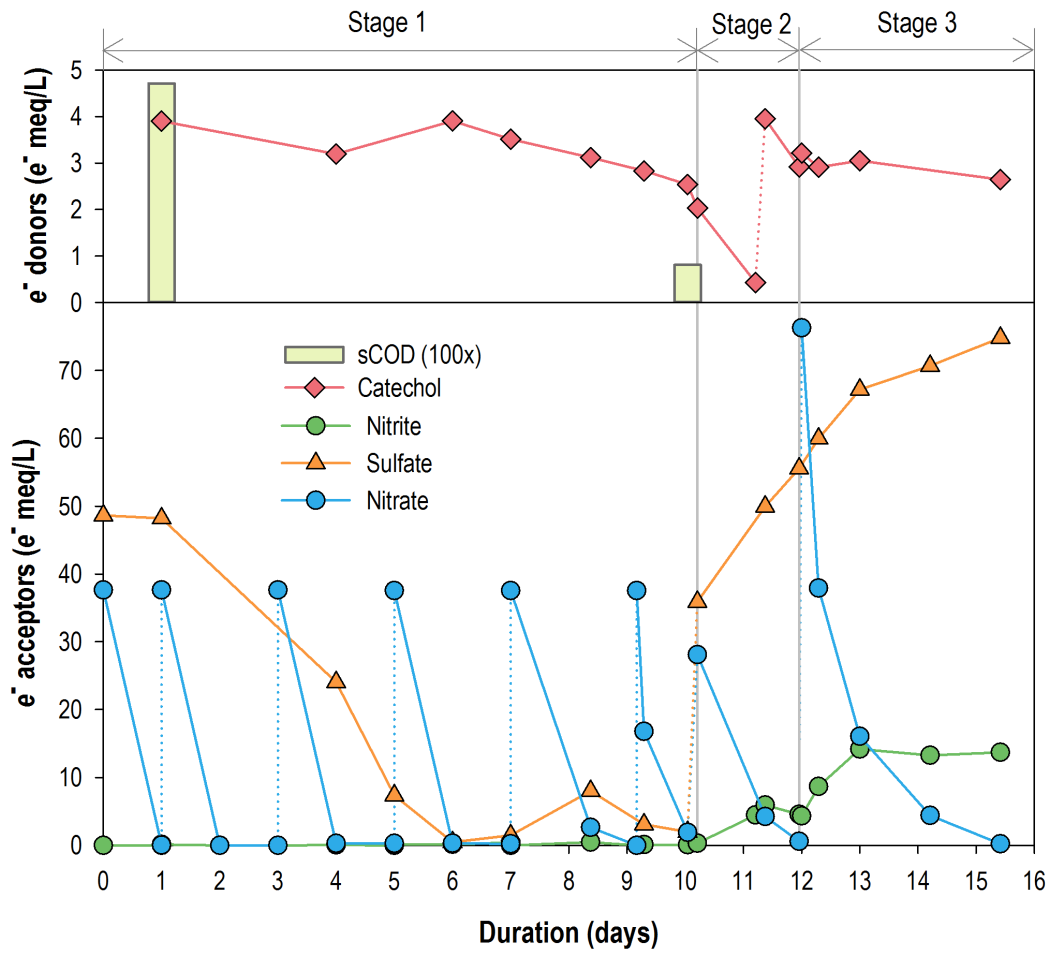

Figure 16. Concentrations of sCOD and catechol (top), as well as electron acceptors (bottom) over repeated feedings of substrates. All concentrations are shown in electron equivalents. The dash lines indicate re-spiking.

In Stage 1 (Day 0 to 10) and coupled with nitrate and sulfate reduction, catechol was gradually utilized along with endogenous COD oxidation after Day 6, and it was consumed up to 50% within the next 4 days (Day 6 to 10). During this stage, over 400 e^- meq/L endogenous COD was consumed with less than 300 e^- meq/L electron-acceptor substrate removal (nitrate and sulfate); the rest of the electrons might have been transferred into biomass synthesis, since the f_s^0 for denitrifiers is around 0.5 with BOD as the electron donor (Rittmann & McCarty, 2001). Sulfate was almost depleted on Day 6, but it rose to 8 e^- meq/L and then decreased again to almost zero on Day 10. This

indicates the possible sulfur cycling happening in the system: SRB reduced sulfate to elemental sulfur or sulfide, and some denitrifiers used sulfur or sulfide as the electron donor and oxidized them to sulfate again. This fate of sulfur suggests that bacteria might have used up most of the favorable electron donors from the endogenous COD, and subsequently they began to use other more resistant electron-donor substrates, such as sulfide or catechol. Thus, this could account for the gradual catechol utilization occurring during this period.

In Stage 2 (Day 10 to 12), catechol showed much faster utilization than in Stage 1, with the other 50% of the initial catechol almost removed in only 1 day and 25% of the re-spiked catechol removed in less than 1 day. Similar to the trend after Day 6, the sulfate concentration kept rising in this stage after a sulfate re-spiking (on Day 10), and the electron equivalents result shows electrons released from sulfide oxidation contributed to 85% of the nitrate reduction. This indicates that sulfide or elemental sulfur became the favorable electron donor in this stage; the previously favorable COD was depleted, and its competitive inhibition to other electron donors was relieved. Thus, the faster utilization of catechol was probably due to favorable COD depletion: only 20% the original COD remained after 10 days, which might be poorly biodegradable substances; with favorable electron donors depleting, bacteria were able to use more resistant substrates, such as catechol, as alternative electron donors. During this stage, nitrite began to accumulate, which further demonstrates limited electron donors that can be easily utilized.

In stage 3, catechol had slower degradation, and its concentration almost stabilized. During this stage, nitrite kept accumulating out to Day 13, although nitrate kept

decreasing to zero at the end of experiment. Again, catechol degradation halted with nitrite accumulation, which is similar to the previous batch experiments and other research (Milligan & Häggblom, 1998), suggesting a catechol-nitrite complex may have some inhibitory impacts on microbial activity on catechol biodegradation. However, the sulfide or sulfur oxidation coupled to nitrate reduction persisted despite nitrite accumulation, indicating the catechol-nitrite complex may only inhibit the catechol-degradation process.

Figure 16 shows the relative abundances of the most abundant microbial phylotypes at the genus level for bacterial samples from the inoculum (noted as "before") and sludge at the end of the experiment (noted as "after"). Overall, the microbial community shifted from dominance by aerobes to dominance by anaerobes. *Janthinobacteria* are strictly aerobic chemoorganotrophs (Gillis & De Ley, 2006); they were at 15% abundance in the inoculum, but did not survive during the anaerobic experiment. Although some species in *Pseudomonas* are facultative denitrifiers, most of them are aerobes; they almost disappeared from the biostimulation column after the 16-day operation. However, an unknown genus in the same family as *Pseudomonas* (family *Pseudomonadaceae*) was enriched with the anaerobic condition, and it was the most abundant group (23.2%), suggesting that other members of the *Pseudomonadaceae* may be responsible for anaerobic biodegradation. A group in family *Porphyromonadaceae* capable of fermentation (Krieg, 2011) was enriched from 0.55% to 13% after anaerobic stimulation, and it may have been mainly responsible for denitrification coupled with oxidations of endogenous COD and the exogenous catechol during the initial 6 days. *Desulfomicrobium* are SRB that could have been responsible for the 50 e^- meq/L sulfate

reduction by Day 10. The *Thiobacillus* group is capable of oxidizing S^{2-}, S^0, and $S_2O_3^{2-}$ coupled with nitrate reduction (Sublette & Sylvester, 1987). Their increase in abundance from 0.16% to 15% after anaerobic stimulation was related to sulfur cycling, and it may account for the continuous sulfate production after Day 10: these bacteria probably used S^{2-}, S^0, or $S_2O_3^{2-}$ from previous sulfate reduction as the electron donors to reduce nitrate, causing sulfate concentration increase.

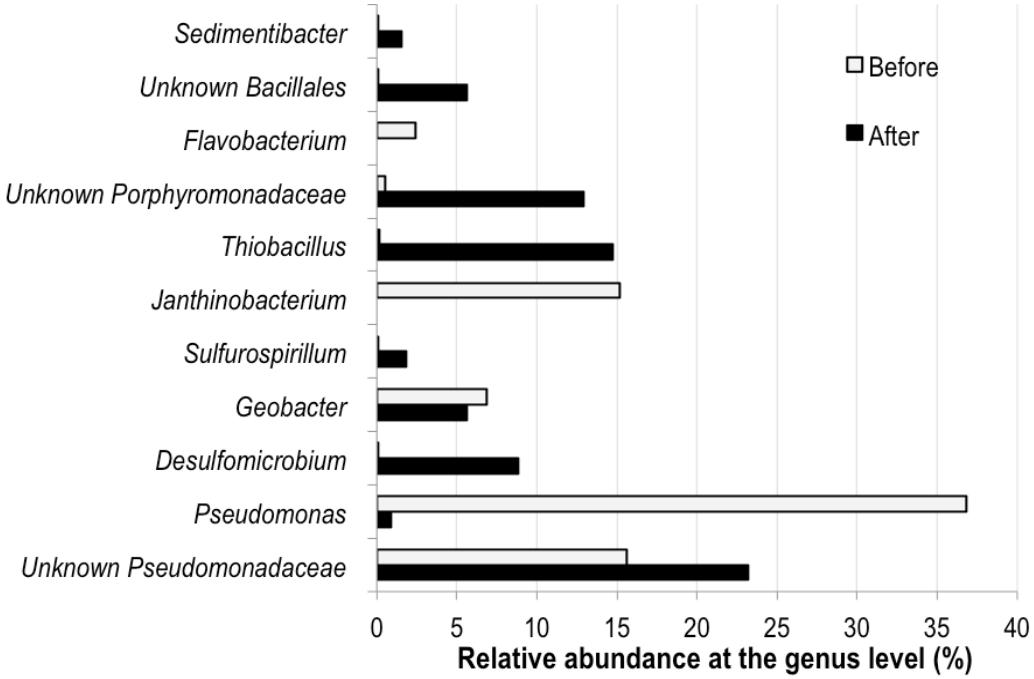

Figure 17. Relative abundances of the most abundant microbial phylotypes at the genus level for bacterial samples from the inoculum (noted as "before") and sludge at the end of the experiment (noted as "after").

5.3 Conclusions

Sulfate- and nitrate-reducing bacteria enriched from a wastewater treatment plant hardly degraded catechol within 20 days. Comparison of substrate and acceptor electron equivalents reveals that electrons from catechol only attributed a small portion of sulfate or nitrate reduction; the bulk of acceptor reduction probably was driven by oxidation of endogenous electron donors, such as organic substances and inorganic S^{2-}/S^0. During

denitrification, nitrite accumulated when electron donor was limited, and it inhibited catechol degradation by forming some toxic catechol-nitrite complex.

In the biostimulation column study with inocula from sites heavily contaminated by petroleum, 90% of the initial 16.5 mg/L catechol, along with endogenous COD, was removed with nitrate- and sulfate-reducing conditions within 11 days. After depletion of endogenous COD, nitrite began accumulating due to the limited electron donor; meanwhile, re-spiked catechol degradation began, but was inhibited by nitrite accumulation probably due to the toxic nitrite-catechol complex.

CHAPTER 6

BENZENE REMOVAL IN AN O_2-BASED MEMBRANE BIOFILM REACTOR

6.1 Experimental Setup

I set up an oxygen-fed MBfR and evaluated it for treating a synthetic groundwater containing benzene and nitrate. I examined benzene removal and intermediates accumulation, and I studied how operational conditions, such as liquid flow rate and oxygen partial pressure in the hollow fibers, affected benzene and nitrate removal performance.

Some materials of our reactor equipment were susceptible to attack by chemicals, which may cause stress cracking, swelling, and oxidation. These reactions may reduce the physical properties of the material, such as destroying fibers' structure that could cause mass loss from the system. Thus, chemical compatibility is of great importance to reactor set-up. I looked up various references for chemicals compatibility guide and summarized the results in Table 4. The numbers shown in the table are average values based on six different reference resources

Table 4. Chemical compatibility guide for benzene and toluene

	Benzene	Toluene
Polypropylene	1.42	1.33
Polyester	0.67	0.87
Polyethylene	1.20	1.30
Polyurethane	1.83	1.83
PTFE (Teflon)	0.00	0.00
Viton	0.14	0.71
Polycarbonate	2.00	2.00

* Chemical compatibility decreases with number increasing.

I did leak tests on polypropylene, polyester, and composite (polyethylene and polyurethane) fibers. I put the fiber into the reactor and filled the reactor with 100 mg/L benzene, and then sampled the reactor for GC analysis every day. Polyester and composite fiber showed good resistance with benzene, but polypropylene fiber was not compatible with benzene, since benzene decreased to below 10% of initial concentration after only 1-day batch, probably due to adsorption. However, although polyester fiber was compatible with benzene, its oxygen delivery capacity is really limited; so I chose composite fiber for oxygen delivering in further experiments.

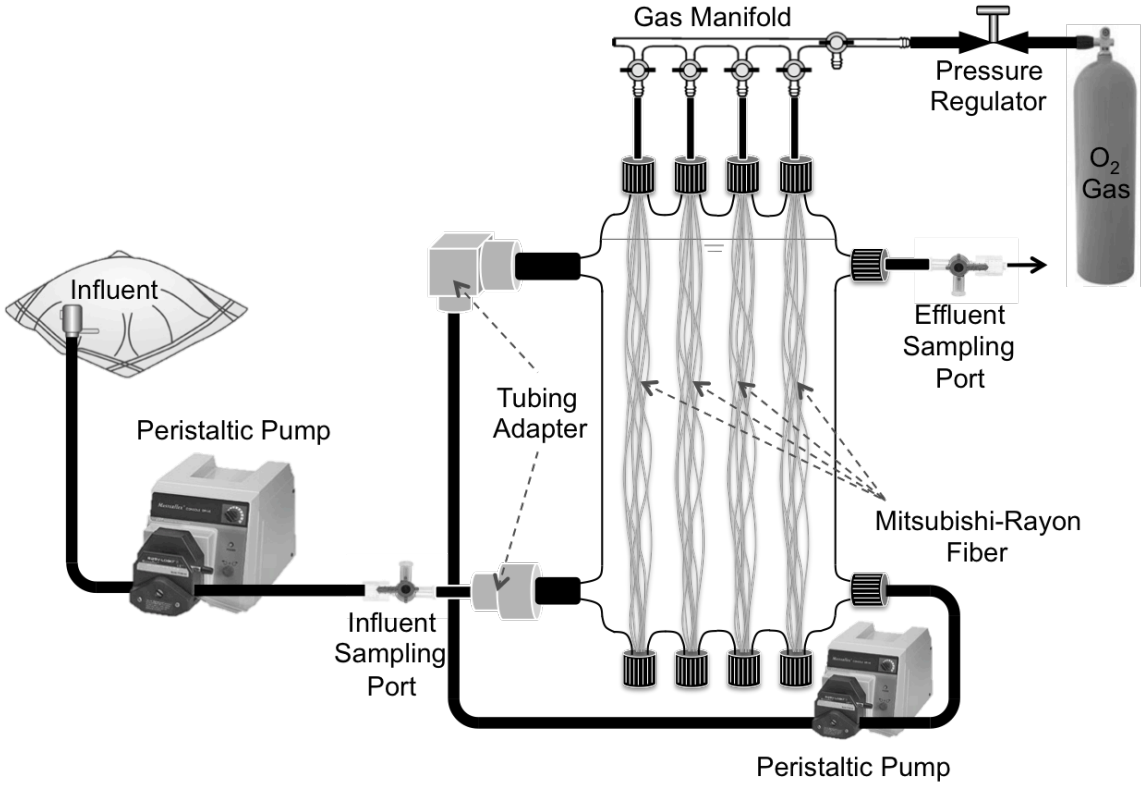

Figure 18. Schematic of the bench-scale MBfR system used in this study to biodegrade benzene with controlled oxygen conditions.

A schematic of the MBfR used in this study is shown in Figure 17. The MBfR system consisted of a glass column, Viton or Teflon tubing, and Teflon stopcocks. The

glass bottle contained four bundles of 32 hollow-fiber membranes (Composite bubble-less gas-transfer membrane, Model MHF 200TL Mitsubishi Rayon Co., Ltd, Tokyo, Japan), each 12 cm long. For each fiber bundle, the top was glued into an O_2-supply manifold, which was connected to gas tank using Norprene tubing, and the bottom was sealed and fixed to the end of the bottle. The MBfR was completely mixed using a high recirculation rate peristaltic pump, which recycled liquid from the bottom to the top of the reactor. A peristaltic pump and Viton tubing provided influent to the MBfR. Before experiment startup, I measured oxygen permeability through the membrane fiber following the method developed by Tang et al. (2012), but replaced the properties of hydrogen gas with the properties of pure oxygen. The physical characteristics of the reactor are provided in Table 5.

Table 5. Physical characteristics of the MBfR system

Characteristics		Units
Number of hollow fibers	128	
Hollow fibers wall thickness	50	μm
Hollow fibers outer diameter	280	μm
Hollow fibers cross-sectional area	61544	μm^2
Hollow fibers length	12	cm
Hollow fibers surface area	110	cm^2
Reactor volume	380	mL
Feed rate	0.08 - 0.12	mL/min
Recirculation rate	150	mL/min

I prepared and stored the feeding medium in a 5-L Tedlar bag (CEL Scientific Corp., Santa Fe Springs, CA). The basic components of medium were consisted of (in mM) 2.5 KH_2PO_4, 2.5 K_2HPO_4, 0.007 $CaCl_2 \cdot 2H_2O$, 0.018 $MgCl_2$, 0.2 NH_4Cl, 0.002 $MgSO_4 \cdot 7H_2O$,

0.002 $FeCl_2 \cdot 4H_2O$, and 4 $NaHCO_3$, plus 1 mL/L trace metal stock solution described by Chung et al. (2006). In addition, considering the potential for two-step aerobic-anaerobic degradation, I added 2.59 mM $NaNO_3$ to the medium as an alternative respirator electron acceptor, which was set on basis of stoichiometry for maximum intermediates anoxic biodegradation. A 5-L glass bottle of deionized water was autoclaved for deoxygenation and sterilization, and it was moved into glove box immediately after autoclaving. DO was maintained below 0.2 mg/L after cooling down, and then all basic medium components were added to the bottle. After transferring the medium from the 5-L glass bottle to a 5-L Tedlar bag inside the glove box, I injected 570 μL pure benzene into the 5-L Tedlar bag using a 1-mL gas-tight syringe (Hamilton Co., Reno, NV) and left it to be completely mixed for at least 24 hours. The final medium pH was 7.1, and the benzene concentration was around 100 mg/L.

After filling the reactor with prepared medium, I inoculated the MBfR with 10 mL of a freshly prepared *Pseudomonas putida* F1 (ATCC 700007) suspension, which was originally purchased from American Type Culture Collection and pre-adapted to benzene and toluene degradation as described in Chapter 4. Upon inoculation, pure O_2 gas was supplied to the lumen of the fibers at 3 psig, and the reactor was operated in recirculation batch mode for 12 h to establish biofilm on the membrane surface. Then, I switched the reactor to continuous mode at a flow rate of 0.08 mL/min (115 mL/d). To determine the effect of flow rate and O_2 partial pressure on the performance of benzene biodegradation, I changed those parameters one-by-one: flow rate from 0.08 to 0.12 mL/min and O_2 partial pressure from 0.4 to 17.7 psi. I changed O_2 partial pressure in the lumen of the fibers by adjusting the pressure regulator or by switching gas tank (pure O_2, air, 2% O_2 +

5% CO_2 balanced by N_2).

The tested oxygen permeability was 6.65×10^{-8} m^3 O_2 @ standard temperature and pressure· m membrane thickness / m^2 fiber surface area · d · bar. The estimated maximum oxygen delivery capacity (meq/m^2-day) was calculated according to permeability tests and formulas derived by Tang et al. (2012). The presumed O_2 flux was calculated based on the needed acceptor flux for sCOD flux beyond nitrate flux and non-soluble biomass:

$$J_{sCOD} = \left(J_{s,N} + J_{s,O}\right)\times\left(1 - f_{BAP}\right) + J_N + J_O \tag{32}$$

where J is the electron equivalent flux, f is the fraction of electrons, subscript s, N, O, and BAP refers to biomass synthesis, nitrate, oxygen, and biomass-associated products, respectively. Equation (32) shows that the sum of nitrate flux, oxygen flux, and flux goes into non-soluble biomass accounts for those electrons released from the actual oxidized electron donor, which is the sCOD flux here. In this equation, $J_{s,N}$ and $J_{s,O}$ can be computed from J_N and J_O:

$$J_{s,N} = \frac{J_N}{1 - f_{s,N} - f_{UAP}}\times f_{s,N} \tag{33}$$

$$J_{s,O} = \frac{J_O}{1 - f_{s,O} - f_{UAP}}\times f_{s,O} \tag{34}$$

where UAP refers to substrate-utilization-associated products. Equation (33) and (34) show that electron acceptor flux accounts for only one part of electron donor flux, and the other two parts are biomass synthesis and UAP. In this calculation, $f_{s,N}$, $f_{s,O}$, f_{UAP}, and f_{BAP} were set at 0.3, 0.54, 0.1, and 0.02, respectively. Substituting Equation (33) and (34) to Equation (32) gives a solution of J_O. In Equation (35), benzene flux is consisted of the

electron fluxes to all electron sinks: electron acceptor, biomass synthesis, degradation intermediates, and UAP.

$$J_{Benzene} = J_N + J_O + J_{s,N} + J_{s,O} + J_{\text{inter}} + J_{UAP} \tag{35}$$

6.2 Results and Discussion

In stage I, pure O_2 was supplied into the lumen of the fibers, and Figure 18 shows the benzene and dissolved oxygen concentrations. During the half day of batch mode, 92% of the initial benzene was removed. Then, I switched it to continuous mode with a flow rate of 0.08 mL/min. After 6 days of continuous operation, benzene removal remained at 99%, and brown-colored solids could be observed on the membrane surface, verifying successful biofilm formation. Figure 19 shows the changes of fiber bundles and bulk liquid turbidity in the MBfR after inoculation.

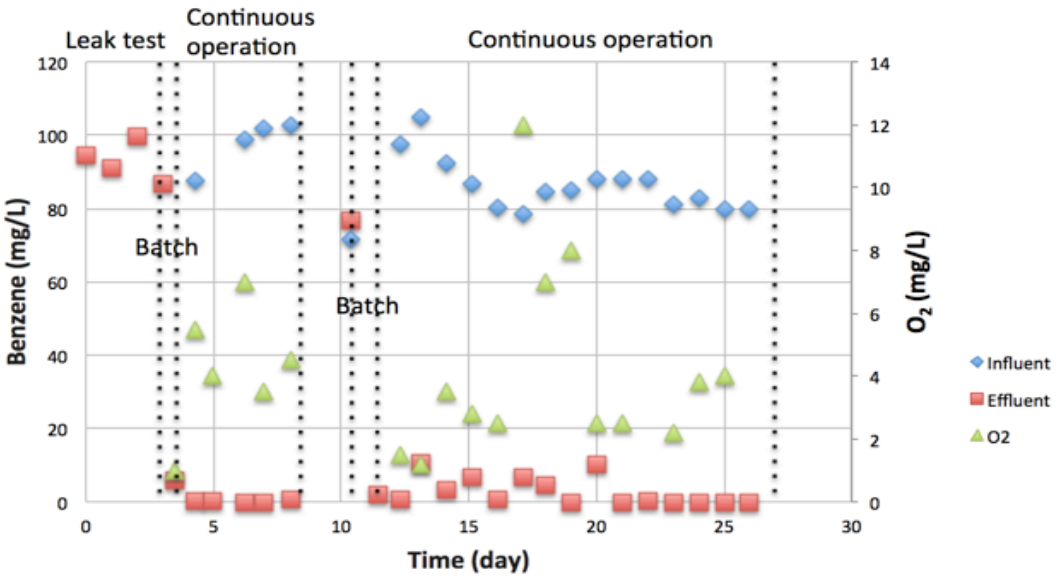

Figure 19. Influent and effluent concentration of benzene, along with effluent dissolved oxygen in stage I.

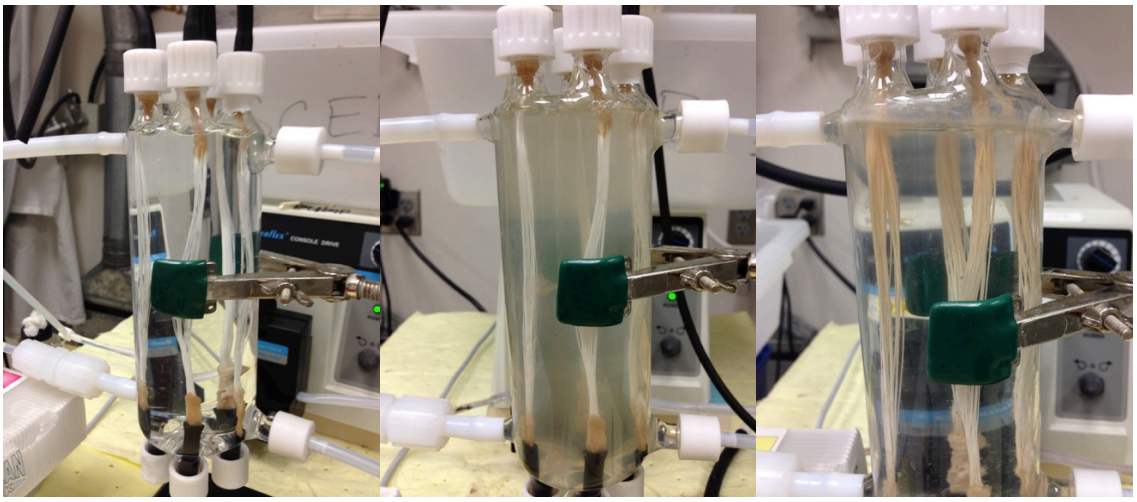

Figure 20. Photograph of the fiber bundles in the MBfR taken before inoculation (left), after inoculation (middle), and 6 days after inoculation (right). The progression from the bright white of the uncolonized fibers to the brown of fibers with biofilm is apparent.

When I increased the flow rate to 0.12 mL/min after another 1 day of batch mode (Day 12), the average benzene removal slightly decreased to 93%, but then rebounded and reached over 99% even when I decreased the pure O_2 pressure from 3 to 2 psig at Day 17. During this stage, the effluent DO was 2 to 4 mg/L, indicating that sufficient oxygen was present in the system to preclude intermediate accumulation; possible intermediates catechol, phenol, and benzoate were not detected by UPLC analyses.

In stage II (Day 26 to 90), air (21% O_2) was supplied to the fibers instead of pure O_2. During this stage, the gas tank pressure was adjusted to 20 psig, 10 psig, and 5 psig in sequence; the ratio of O_2 partial pressure for 20 : 10 : 5 psig was 1.76 : 1.25 : 1.

Figure 20 summarizes the results for benzene when air was delivered to the fibers. Effluent benzene increased shortly after the change in O_2 pressure, and it reached a steady state with 71% benzene removal after 10-days of continuous operation. Then, I changed the flow rate from 0.12 to 0.10 mL/min, which resulted in effluent benzene concentration decreasing to give 95% removal after 10 days. When I continued to lower

the gas pressure to 10 psig and 5 psig without changing any other parameters, the effluent benzene concentration increased and reached steady states with 71% and 55% removal, respectively. These results demonstrate that O_2 availability strongly affected the kinetics of benzene biodegradation. In addition, effluent pH was lower than the pH of the influent, indicating net proton production during benzene biodegradation, which is consistent with the stoichiometry in Equation 23.

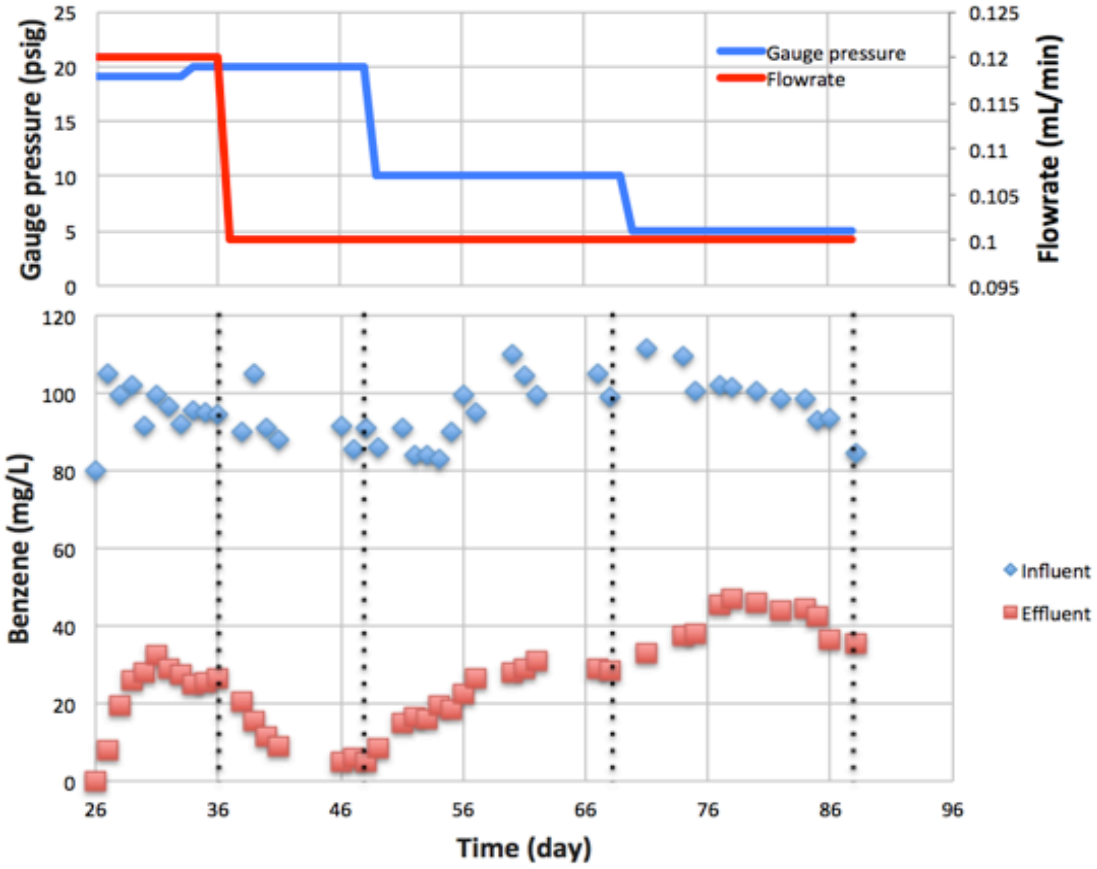

Figure 21. Influent and effluent concentration of benzene, along with flow rate and gauge pressure in stage II

During Stage II, the effluent DO always was below 1 mg/L, favoring intermediate accumulation, as observed in our previous experiments (Chapter 4). However, UPLC did not detect intermediates in the effluent. The differences between this experiment and our

previous experiments are listed in Table 6. In our previous batch experiments, bacteria grew in suspension in a completely mixed condition, with ~ 0.6 mg/L DO. In the MBfR, in contrast, bacteria mainly grew on the surface of the fiber, where oxygen was relatively abundant due to direct delivery. Thus, although the dissolved oxygen concentration I measured in the bulk liquid was below 1 mg/L, the biofilm bacteria could be exposed to a higher concentration.

Table 6. Differences between this MBfR and previous experiments

Differences	This experiment	Previous batch experiment
Reactor	Continuous well-mixed membrane biofilm reactor	Completely-mixed batch reactor
Gas supplied	Air	2%O_2+5%CO_2 balanced with N_2
Gas supply methods	Diffusion through membrane	Diffusion from headspace
Bacteria distribution	Mainly on the membrane	Suspended

In Stage III (from Day 90), I changed the supplied gas from air to 2% O_2, 5% CO_2, and 93% N_2. Figure 21 presents the experimental results. Two accidents happened during this stage. First, the influent was accidently turned off at Day 91, and the reactor was in batch mode for four days, at which time the benzene concentration decreased almost to zero. Second, the recirculation tubing broke at Day 102, and the reactor was emptied; I refilled the reactor with medium within 12 hours of the breakage. The effluent benzene concentration reached a steady state with 48% benzene removal after 15 days of continuous operation.

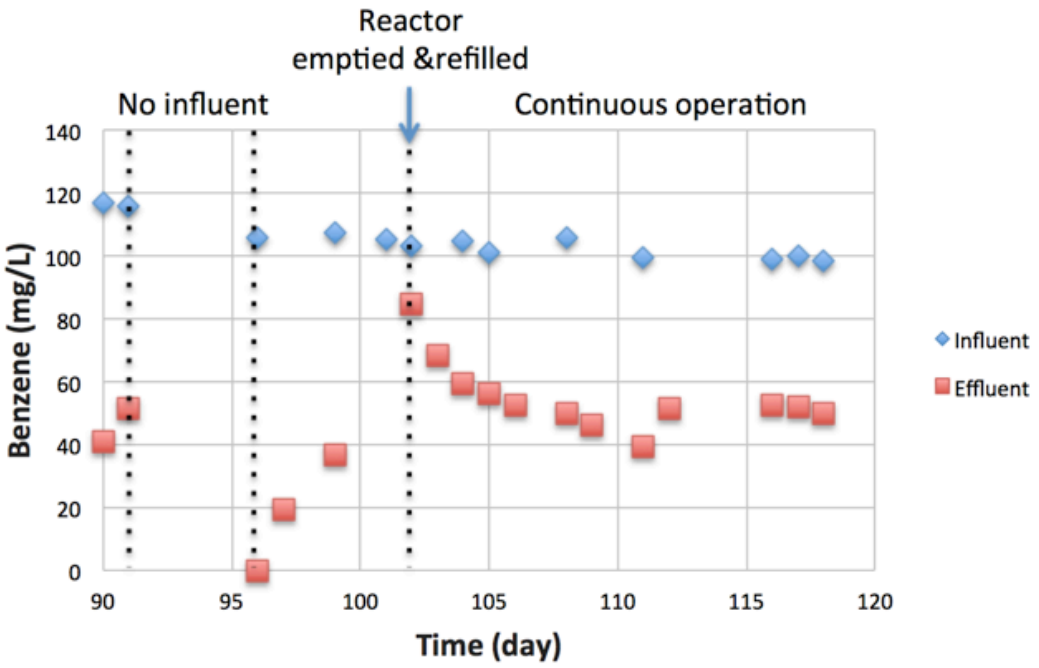

Figure 22. Influent and effluent concentration of benzene in Stage III.

Table 7 summarizes the operational parameters, benzene concentration, and calculated benzene removal performance for the seven steady states in Stages I, II, and III. Included in the table are hydraulic retention time (HRT), benzene surface loading, benzene removal flux, effluent benzene concentration, benzene removal ratio, and benzene removal rate. The benzene flux and effluent concentration ranged from 0.6 to 1.3 g/m^2 of biofilm surface area/day and 0.2 to 51.6 mg/L, respectively. Oxygen availability controlled the effluent benzene concentration and benzene flux: lower O_2 availability slowed less benzene removal, but I did not detect di-oxygenation intermediates in any case.

Table 7. The average performance parameters at eight steady states in stage I, II and III

Stage	Flow rate	HRT	Gas supplied	Gauge pressure (O_2 partial pressure)	pH_{inf} (pH_{eff})	$Benzene_{eff}$	Benzene surface loading	Benzene removal		
								flux	ratio	rate
	mL/min	day		psig (psi)		mg/L	g/m^2-day		%	mg/day
I	0.08	3.3	Pure O_2	3 (17.7)	--	0.2	1.1	1.1	99	11.6
	0.12	2.2	Pure O_2	3 (17.7)	--	3.6	1.4	1.3	94	14.3
	0.12	2.2	Pure O_2	2 (16.7)	--	0.3	1.3	1.3	99	14.0
II	0.12	2.2	Air	20 (7.3)	6.80 (6.43)	25.8	1.5	1.1	74	12.0
	0.10	2.6	Air	20 (7.3)	6.79 (6.43)	5.5	1.2	1.1	94	12.1
	0.10	2.6	Air	10 (5.2)	7.09 (6.90)	29.6	1.3	0.9	71	10.3
	0.10	2.6	Air	5 (4.1)	7.11 (6.98)	43.8	1.2	0.7	54	7.7
III	0.10	2.6	2% O_2	15 (0.59)	7.25 (7.06)	51.6	1.3	0.6	48	6.9

The electron equivalent fluxes of electron donors – benzene, sCOD – and electron acceptors – nitrate, oxygen – are summarized in Table 8. In stage I, the presumed O_2 fluxes were always lower than the maximum O_2 fluxes, indicating sufficient O_2 supply, and this can explain the abundant DO in the effluent during this stage. In Stage II, the presumed O_2 flux was higher than the maximum O_2 flux in experiment 4, 5, and 6. This suggests underestimating maximum O_2 flux or overestimating the presumed O_2 flux. Over these experiments, I observed the composite fibers used in this study did not remain bubbleless, as small bubbles formed on the surface of the fibers. Thus, this might be the reason causing underestimation of maximum O_2 flux in experiment 4, 5, and 6.

Table 8. Electron-equivalent fluxes at eight steady states in Stages I, II and III. Electron-equivalent flux was calculated as described in Chapter 2.4. sCOD were measured values across the MBfR.

Stage	EXP[a]	Benzene	sCOD	Nitrate	Estimated Max O_2	Presumed O_2 [b]
		Flux in e^- meq/m^2-day				
I	1	406	--[c]	0	290	164[d]
	2	500	--[c]	0	290	202[d]
	3	490	--[c]	0	273	198[d]
II	4	417	345	23	119	170
	5	422	413	51	119	144
	6	360	347	74	85	93
	7	270	182	74	68	51
III	8	240	214	99	10	12

[a] EXP is short for "experiment."
[b] Calculated by Equation (32), (33), and (34)
[c] Data are not available.
[d] Calculated by assuming benzene flux equals sCOD flux.

Figure 22 shows the potential electron flow for electron donors in this system. I assumed the influent benzene electron equivalents equaled to sCOD electron equivalents,

which was consistent with measured benzene concentration and sCOD value. Thus, the relationships among different fluxes are:

$$\text{Benzene Flux} = \text{Benzene}_{\text{inf}} - \text{Benzene}_{\text{eff}} = e_1^- - e_2^-$$

$$\text{sCOD Flux} = \text{sCOD}_{\text{inf}} - \text{sCOD}_{\text{eff}} = e_1^- - (e_2^- + e_3^-)$$

➔ $\text{SMP + Intermediates Flux} = \text{Benzene Flux} - \text{sCOD Flux} = e_3^-$

the difference between benzene flux and sCOD flux represents the SMP and degradation intermediates. In Table 8, benzene flux was larger than sCOD flux in experiment 4 to 8, indicating that SMP and intermediates were in the effluent.

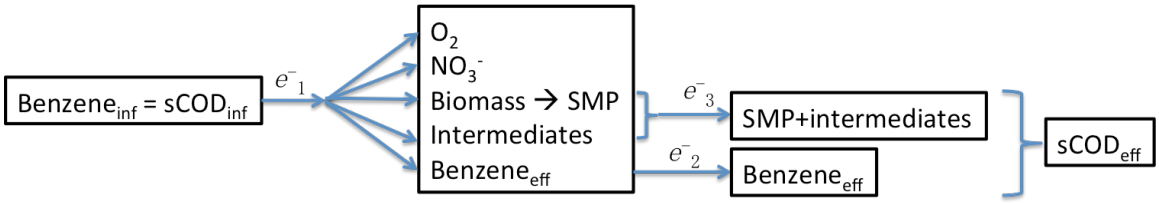

Figure 23. Electron flow for electron donors.

Based on the model developed by Equations (32) to (35), Figure 23 shows the modeled electron-equivalent fluxes distributed among different electron sinks over experiment 4 to 8. The nitrate flux increased as the O_2 delivery flux decreased, supporting that O_2 availability controlled the nitrate flux. Although the inoculum was pure *Pseudomonas putida* F1 strain, I did not keep the whole system sterile throughout operation; thus, microorganisms other than *Pseudomonas putida* F1 were present in the MBfR. As a result of this, the nitrate flux increased after the gas supply was switched from pure O_2 to air (Table 8). As O_2 availability decreasing (DO < 1mg/L after Stage I), denitrification became more important than aerobic respiration, as confirmed by a larger nitrate flux and a smaller O_2 flux. At the end of operation (EXP 8), nitrate reduction accounted for most of the electrons released from benzene, but oxygen reduction also was

an electron sink, at a minimum for activation of the benzene ring. When oxygen was the dominant electron acceptor, biomass synthesis accounted for a large portion of electrons released from benzene oxidation, especially those through aerobic respiration, corresponding to its f_s value (0.54). In addition, intermediates and SMP accounted for a fraction of electron flux, which was the difference between benzene flux and sCOD flux.

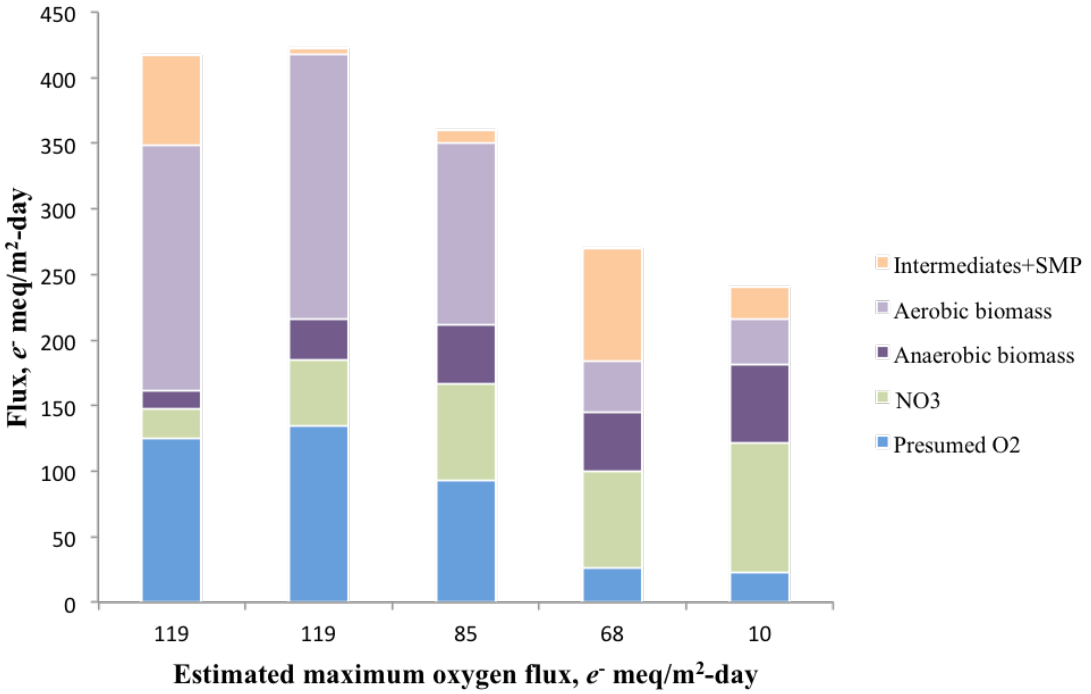

Figure 24. Modeled electron-equivalent fluxes distribution among nitrate, O_2, biomass, and intermediates plus SMP over experiment 4 to 8. The total height of each bar indicates benzene flux; intermediate plus SMP was calculated by Equation (35).

Although benzene has been considered persistent in anaerobic conditions, anaerobic benzene degradation coupled to nitrate reduction has been demonstrated in enrichment and pure cultures (Burland & Edwards, 1999; Coates et al., 2001; Kasai et al., 2006; Ulrich & Edwards, 2003). Thus, it is possible that denitrifiers used benzene directly as an electron donor to reduce nitrate, or they used intermediates after benzene was activated by di-oxygenation. In order to explore what bacteria were present in the biofilm and

what they were doing, I sampled the biofilm after stage III (Figure 24) for microbial community analyses.

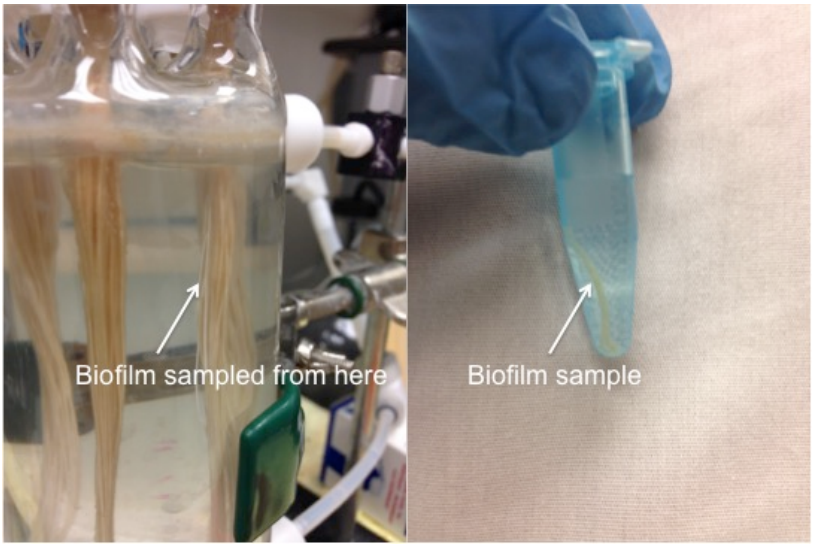

Figure 25. Photograph of biofilm sample, taken after Stage III.

Figure 25 presents the relative microbial abundances for the biofilm sample. The initially inoculated *Pseudomonas* strain was only 0.36% of the biofilm community after 120-days of continuous operation. Instead, the microbial community was dominated by the family *Comamonadaceae* (58%), which includes the genera *Comamonas*, *Polaromonas*, *Acidovorax*, *Hydrogenophaga*, *Xylophilus* and *Variovorax*. Many aerobic benzene-degrading isolates have been identified in genera *Hydrogenophaga* (Fahy et al., 2008) and *Comamonas* (Jiang et al., 2014), and abundant species in aerobic benzene-degrading microcosm have been identified as *Acidovorax* (Fahy et al., 2006), *Polaromonas* (Xie et al., 2011), and *Variovorax* (Rooney-Varga et al., 1999). Besides, *Comamonadaceae* was also found capable of denitrification with low oxygen supply (Sadaie et al., 2007). Thus, with such a huge abundance and known characteristics of aerobic benzene degradation and denitrification, *Comamonadaceae* probably was

responsible for the benzene removal in this MBfR system, featuring aerobic activation reactions and then complete mineralization coupled to nitrate reduction.

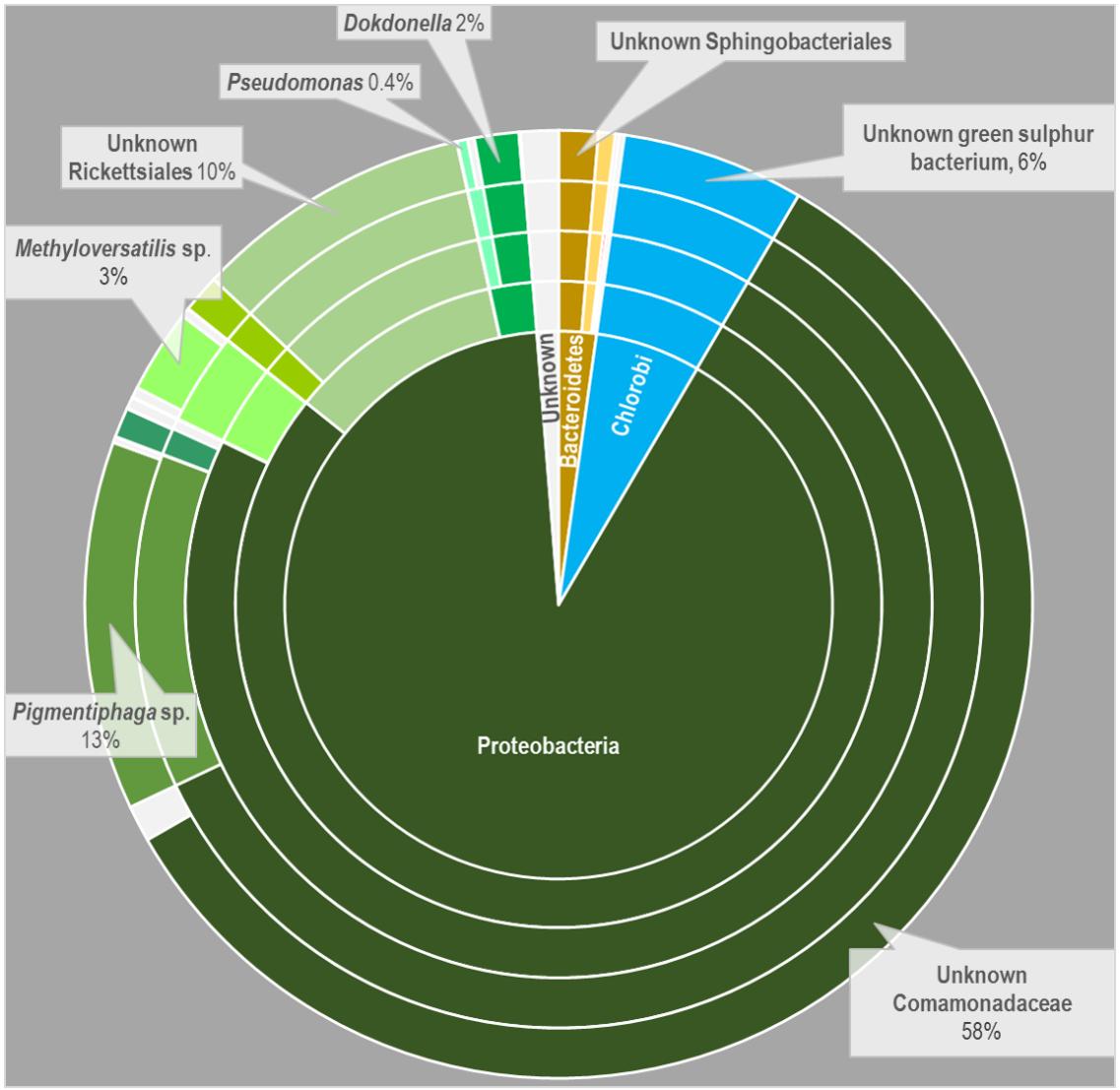

Figure 26. Relative microbial abundance at phylum, class, order, family and genus levels for the MBfR biofilm sample.

Pigmentiphaga sp. (13% abundance) in the family *Alcaligenaceae* was reported to aerobically degrade aromatic or long-chain hydrocarbon compounds (Kubota et al., 2008; Yang et al., 2013), and it may also have been responsible for aerobic benzene oxidation in the MBfR. Family *Rhodocyclaceae* (3.5% abundance) was reported being responsible

for anaerobic benzene degradation under denitrifying conditions (van der Zaan et al., 2012), and it could have contributed to benzene degradation coupled with nitrate reduction in this MBfR. *Chlorobi* (6% abundance), also known as green sulfur bacteria, surprisingly were presented in the benzene-degrading MBfR system. Green sulfur bacteria are obligate photolithotrophs, which carry out anaerobic photosynthesis using hydrogen sulfide as electron donor and light energy to create organic compound. This bacteria and the exposure to light could account for 0.2 mg/L sulfate increase from the effluent.

6.3 Conclusions

In this chapter, I describe the performance of the O_2-based MBfR for removing benzene from a synthetic groundwater with low levels of dissolved oxygen. The results demonstrate that it was possible to bioremediate benzene-contaminated water in the MBfR and in micro-aerobic conditions.

At an average benzene surface loading of 1.3 g/m^2-day and an average flow rate of 0.12 mL/min (2.2-day HRT), the MBfR supplied with pure O_2 successfully achieved 99% benzene removal at steady state. With lower oxygen partial pressure, benzene removal fluxes decreased, while nitrate fluxes increased, indicating multiple mechanisms, including oxygenation and nitrate reduction, were involved in the system under oxygen-limiting conditions.

Microbial community analysis results reveal that, although the originally inoculated *Pseudomonas* almost disappeared from the system, strains from the family *Comamonadaceae* became the most abundant bacteria present in the biofilm and probably contributed to benzene biodegradation in a major way.

CHAPTER 7

SUMMARY AND RECOMMENDATIONS

7.1 Summary

For *in situ* bioremediation, the lack of dissolved oxygen in groundwater usually limits benzene and toluene removals. In my batch experiments for benzene and toluene anaerobic degradation, the inoculum was able to biodegrade toluene coupled to sulfate reduction in the presence of benzene, but benzene biodegradation was minimal.

When oxygen was present, toluene and benzene were effectively biodegraded by *Pseudomonas putida* F1. Based on electron and energy balances involved in oxygenation reactions, I developed stoichiometry equations to describe the biological reactions. Adding di-oxygenation reactions as activation steps lowers the overall yield for full mineralization, and it also may delay synthesis if intermediates accumulate. When DO was depleted, a half-open batch experiment demonstrated accumulation of di-oxygenation intermediates during aerobic biodegradation, but a stable oxygen-limiting condition was impractical for me to maintain. I developed a two-step model to link biomass growth to the substrate utilization; the modeling results were identical to the experimental results during the first-half of the experiment, although they deviated later due to medium color. A lag in biomass production, continued biomass growth after complete substrate removal, and two-step modeling results all supported biomass synthesis was tied to oxidation of di-oxygenation intermediates.

I conducted batch experiments and a biostimulation column study on catechol, which was the first di-oxygenation intermediate from benzene and accumulated under oxygen-liming condition, to see if it could be further degraded through the anaerobic

pathway. Inoculum from petroleum-contaminated site was able to degrade catechol along with endogenous COD oxidation coupled to nitrate reduction. However, catechol degradation slowed down with nitrite accumulation, probably due to the inhibitory impact of the catechol-nitrite complex on microbial activity during catechol degradation process.

Because bubbling aeration is energy intensive and can lead to benzene vapor emission, membrane aeration is a good way to supply oxygen economically and efficiently. With an average benzene surface loading of 1.3 g/m^2-day and an average flow rate of 0.12 mL/min (2.2-day HRT), an MBfR supplied with pure O_2 successfully achieved 99% benzene removal at steady state with residual DO. With lower oxygen partial pressure, benzene removal fluxes decreased, while nitrate fluxes increased, indicating multiple mechanisms, including oxygenation and nitrate reduction, were involved in the system under oxygen-limiting conditions. After 120-days continuous operation, the original inoculated *Pseudomonas* species did not persist; instead, the family *Comamonadaceae* dominated the biofilm and probably contributed to benzene biodegradation in a major way with aerobic activation reactions and then complete mineralization coupled to nitrate reduction.

7.2 Recommendations for Future Study

Nitrate and oxygen are the potential electron acceptors present in the MBfR system. Conducting control experiments by taking either oxygen or nitrate out of the system is a good way to analyze their influence on each other. Meanwhile, deeper microbial community analysis can also help us to find out the syntrophic relationship among different bacteria.

Although benzene and toluene are typical and important aromatic contaminants,

many other compounds like ethylbenzene and xylenes (the E and X of BTEX) often also are present in gasoline-contaminated groundwater. Thus, more contaminants should be tested alone and coexisting with benzene and toluene. It is especially worthwhile to identify inhibition (or possibly stimulation) effects of the different compounds to each other.

Although it will be a long road for applying the O_2-based MBfR to *in situ* groundwater remediation, the reactor could be scaled up to test its feasibility. A 2-D tank packed with filler can be used to simulate aquifer environmental, and bundles of the fiber can be inserted into the tank from the top to supply oxygen to the 'closed system'. Synthetic BTEX-contaminated groundwater can flow through the tank at constant flow rate from one side to another side. The goal is to document the performance of oxygen delivery and contaminants removal rate for setting in which the BTEX components coexist. Of particular interest would be simulating the dissolution and biodegradation of BTEX from a non-aqueous phase.

REFERENCES

Aburto, A., Fahy, A., Coulon, F., Lethbridge, G., Timmis, K., Ball, A.S. & McGenity, T.J. (2009), Mixed aerobic and anaerobic microbial communities in benzene‐contaminated groundwater. Journal of applied microbiology 106(1), 317-328.

Aihara, J. (1992), Why Aromatic-Compounds Are Stable. Scientific American 266(3), 62-68.

Anderson, R.T. & Lovley, D.R. (1997), Advances in microbial ecology, pp. 289-350, Springer.

Aronson, D. & Howard, P.H. (1997), Anaerobic biodegradation of organic chemicals in groundwater: a summary of field and laboratory studies, Environmental Science Center, Syracuse Research Corporation.

Beller, H.R., Grbicgalic, D. & Reinhard, M. (1992), Microbial Degradation of Toluene under Sulfate-Reducing Conditions and the Influence of Iron on the Process. Applied and Environmental Microbiology 58(3), 786-793.

Buchdahl, R., Willems, C.D., Vander, M. & Babiker, A. (2000), Associations between ambient ozone, hydrocarbons, and childhood wheezy episodes: a prospective observational study in south east London. Occupational and environmental medicine 57(2), 86-93.

Burland, S.M. & Edwards, E.A. (1999), Anaerobic benzene biodegradation linked to nitrate reduction. Applied and environmental microbiology 65(2), 529-533.

Caldwell, M.E. & Suflita, J.M. (2000), Detection of phenol and benzoate as intermediates of anaerobic benzene biodegradation under different terminal electron-accepting conditions. Environmental science & technology 34(7), 1216-1220.

Caporaso, J.G., Kuczynski, J., Stombaugh, J., Bittinger, K., Bushman, F.D., Costello, E.K., Fierer, N., Pena, A.G., Goodrich, J.K., Gordon, J.I., Huttley, G.A., Kelley, S.T., Knights, D., Koenig, J.E., Ley, R.E., Lozupone, C.A., McDonald, D., Muegge, B.D., Pirrung, M., Reeder, J., Sevinsky, J.R., Tumbaugh, P.J., Walters, W.A., Widmann, J., Yatsunenko, T., Zaneveld, J. & Knight, R. (2010), QIIME allows analysis of high-throughput community sequencing data. Nature Methods 7(5), 335-336.

Caporaso, J.G., Lauber, C.L., Walters, W.A., Berg-Lyons, D., Huntley, J., Fierer, N., Owens, S.M., Betley, J., Fraser, L. & Bauer, M. (2012), Ultra-high-throughput microbial community analysis on the Illumina HiSeq and MiSeq platforms. The ISME journal 6(8), 1621-1624.

Centers for Disease Control (1994), Continued use of drinking water wells contaminated with hazardous chemical substances--Virgin Islands and Minnesota, 1981-1993. MMWR. Morbidity and mortality weekly report 43(5), 89.

Chakraborty, R. & Coates, J.D. (2005), Hydroxylation and carboxylation—two crucial steps of anaerobic benzene degradation by Dechloromonas strain RCB. Applied and environmental microbiology 71(9), 5427-5432.

Chang, M.-K., Voice, T.C. & Criddle, C.S. (1993), Kinetics of competitive inhibition and cometabolism in the biodegradation of benzene, toluene, and p-xylene by two Pseudomonas isolates. Biotechnology and Bioengineering 41(11), 1057-1065.

Chiang, C., Salanitro, J., Chai, E., Colthart, J. & Klein, C. (1989), Aerobic biodegradation of benzene, toluene, and xylene in a sandy aquifer—data analysis and computer modeling. Groundwater 27(6), 823-834.

Christensen, T.H., Bjerg, P.L., Banwart, S.A., Jakobsen, R., Heron, G. & Albrechtsen, H.-J. (2000), Characterization of redox conditions in groundwater contaminant plumes. Journal of Contaminant Hydrology 45(3), 165-241.

Christensen, T.H., Kjeldsen, P., Bjerg, P.L., Jensen, D.L., Christensen, J.B., Baun, A., Albrechtsen, H.-J. & Heron, G. (2001), Biogeochemistry of landfill leachate plumes. Applied Geochemistry 16(7), 659-718.

Chung, J., Nerenberg, R. & Rittmann, B.E. (2006), Bioreduction of selenate using a hydrogen-based membrane biofilm reactor. Environmental science & technology 40(5), 1664-1671.

Coates, J.D., Chakraborty, R., Lack, J.G., O'Connor, S.M., Cole, K.A., Bender, K.S. & Achenbach, L.A. (2001), Anaerobic benzene oxidation coupled to nitrate reduction in pure culture by two strains of Dechloromonas. Nature 411(6841), 1039-1043.

Cohen-Bazire, G., Sistrom, W.R. & Stanier, R.Y. (1957), Kinetic studies of pigment synthesis by non-sulfur purple bacteria. J Cell Physiol 49(1), 25-68.

Colberg, P.J. & Young, L.Y. (1995), Anaerobic degradation of nonhalogenated homocyclic aromatic compounds coupled with nitrate, iron, or sulfate reduction. Microbial transformation and degradation of toxic organic chemicals 307330.

Crawford, D.W., Bonnevie, N.L. & Wenning, R.J. (1995), Sources of pollution and sediment contamination in Newark Bay, New Jersey. Ecotoxicology and Environmental Safety 30(1), 85-100.

Dahlen, E.P. & Rittmann, B.E. (2000), Analysis of oxygenation reactions in a multi-substrate system - A new approach for estimating substrate-specific true yields. Biotechnology and Bioengineering 70(6), 685-692.

Davis, E., Murray, H., Liehr, J. & Powers, E. (1981), Basic microbial degradation rates and chemical byproducts of selected organic compounds. Water Res 15(9), 1125-1127.

Davis, J.W., Klier, N.J. & Carpenter, C.L. (1994), Natural biological attenuation of benzene in ground water beneath a manufacturing facility. Groundwater 32(2), 215-226.

Delfino, R.J., Gong Jr, H., Linn, W.S., Pellizzari, E.D. & Hu, Y. (2003), Asthma symptoms in Hispanic children and daily ambient exposures to toxic and criteria air pollutants. Environmental health perspectives 111(4), 647.

Ding, B., Schmeling, S. & Fuchs, G. (2008), Anaerobic metabolism of catechol by the denitrifying bacterium Thauera aromatica—A result of promiscuous enzymes and regulators? J Bacteriol 190(5), 1620-1630.

Dou, J., Liu, X., Hu, Z. & Deng, D. (2008a), Anaerobic BTEX biodegradation linked to nitrate and sulfate reduction. Journal of Hazardous Materials 151(2), 720-729.

Dou, J.F., Liu, X., Hu, Z.F. & Deng, D. (2008b), Anaerobic BTEX biodegradation linked to nitrate and sulfate reduction. Journal of Hazardous Materials 151(2-3), 720-729.

Fahy, A., Ball, A.S., Lethbridge, G., Timmis, K. & McGenity, T.J. (2008), Isolation of alkali‐tolerant benzene‐degrading bacteria from a contaminated aquifer. Letters in applied microbiology 47(1), 60-66.

Fahy, A., McGenity, T.J., Timmis, K.N. & Ball, A.S. (2006), Heterogeneous aerobic benzene-degrading communities in oxygen-depleted groundwaters. FEMS microbiology ecology 58(2), 260-270.

Foght, J. (2008), Anaerobic biodegradation of aromatic hydrocarbons: Pathways and prospects. Journal of Molecular Microbiology and Biotechnology 15(2-3), 93-120.

Gibson & Subramanian (1984), Microbial degradation of aromatic hydrocarbons, Marcel Dekker, Inc., New York.

Gibson, D., Koch, J. & Kallio, R. (1968), Oxidative degradation of aromatic hydrocarbons by microorganisms. I. Enzymic formation of catechol from benzene. Biochemistry 7(7), 2653-2662.

Gibson, D., Zylstra, G. & Chauhan, S. (1990), Biotransformations catalyzed by toluene dioxygenase from Pseudomonas putida F 1.

Gibson, D.T., Hensley, M., Yoshioka, H. & Mabry, T.J. (1970), Formation of (+)-Cis-2,3-Dihydroxy-1-Methylcyclohexa-4,6-Diene from Toluene by Pseudomonas-Putida. Biochemistry 9(7), 1626-&.

Gillis, M. & De Ley, J. (2006), The Genera Chromobacterium and Janthinobacterium. The Prokaryotes: Volume 5: Proteobacteria: Alpha and Beta Subclasses, 737-746.

Gorny, N. & Schink, B. (1994), Anaerobic degradation of catechol by Desulfobacterium sp. strain Cat2 proceeds via carboxylation to protocatechuate. Applied and environmental microbiology 60(9), 3396-3400.

Jiang, B., Zhou, Z., Dong, Y., Tao, W., Wang, B., Jiang, J. & Guan, X. (2014), Biodegradation of benzene, toluene, ethylbenzene, and o-, m-, and p-xylenes by the newly isolated bacterium Comamonas sp. JB. Applied Biochemistry and Biotechnology, 1-9.

Jindrova, E., Chocova, M., Demnerova, K. & Brenner, V. (2002), Bacterial aerobic degradation of benzene, toluene, ethylbenzene and xylene. Folia Microbiologica 47(2), 83-93.

Kasai, Y., Takahata, Y., Manefield, M. & Watanabe, K. (2006), RNA-based stable isotope probing and isolation of anaerobic benzene-degrading bacteria from gasoline-contaminated groundwater. Applied and environmental microbiology 72(5), 3586-3592.

Keller, K.A. & Snyder, C.A. (1988), Mice exposed in utero to 20 ppm benzene exhibit altered numbers of recognizable hematopoietic cells up to seven weeks after exposure. Toxicological Sciences 10(2), 224-232.

Krieg, N. (2011), Family IV. Porphyromonadaceae fam. nov. Bergey's manual of systematic bacteriology 4.

Kubota, K., Koma, D., Matsumiya, Y., Chung, S.-Y. & Kubo, M. (2008), Phylogenetic analysis of long-chain hydrocarbon-degrading bacteria and evaluation of their hydrocarbon-degradation by the 2, 6-DCPIP assay. Biodegradation 19(5), 749-757.

Kukor, J.J. & Olsen, R.H. (1991), Genetic organization and regulation of a meta cleavage pathway for catechols produced from catabolism of toluene, benzene, phenol, and cresols by Pseudomonas pickettii PKO1. J Bacteriol 173(15), 4587-4594.

Lovley, D.R. (2001), Anaerobes to the rescue. Science 293(5534), 1444-1446.

Lovley, D.R. (1997), Potential for anaerobic bioremediation of BTEX in petroleum-contaminated aquifers. Journal of Industrial Microbiology & Biotechnology 18(2-3), 75-81.

Madigan, Martinko & Parker (2000), Brock Biology of Microorganisms, Prentice-Hall, Inc., New York.

Majora, D.W., Mayfielda, C.I. & Barkerb, J.F. (1988), Biotransformation of benzene by denitrification in aquifer sand. Groundwater 26(1), 8-14.

Martin, K.J. & Nerenberg, R. (2012), The membrane biofilm reactor (MBfR) for water and wastewater treatment: principles, applications, and recent developments. Bioresour Technol 122, 83-94.

Mavrovouniotis, M.L. (1991), Estimation of standard Gibbs energy changes of biotransformations. Journal of Biological Chemistry 266(22), 14440-14445.

Mavrovouniotis, M.L. (1990), Group contributions for estimating standard gibbs energies of formation of biochemical compounds in aqueous solution. Biotechnol Bioeng 36(10), 1070-1082.

Merchant Reaearch & Consulting ltd (2015), Benzene: 2015 World Market Outlook and Forecast up to 2019. http://mcgroup.co.uk/news/20140502/benzene-production-exceed-5095-mln-tonnes.html.

Milligan, P.W. & Häggblom, M.M. (1998), Biodegradation of resorcinol and catechol by denitrifying enrichment cultures. Environmental toxicology and chemistry 17(8), 1456-1461.

Nicolai, T., Carr, D., Weiland, S., Duhme, H., Von Ehrenstein, O., Wagner, C. & Von Mutius, E. (2003), Urban traffic and pollutant exposure related to respiratory outcomes and atopy in a large sample of children. European respiratory journal 21(6), 956-963.

Ontiveros-Valencia, A., Tang, Y., Krajmalnik-Brown, R. & Rittmann, B.E. (2014), Managing the interactions between sulfate-and perchlorate-reducing bacteria when using hydrogen-fed biofilms to treat a groundwater with a high perchlorate concentration. Water Research 55, 215-224.

Ontiveros-Valencia, A., Ziv-El, M., Zhao, H.-P., Feng, L., Rittmann, B.E. & Krajmalnik-Brown, R. (2012), Interactions between nitrate-reducing and sulfate-reducing bacteria coexisting in a hydrogen-fed biofilm. Environmental science & technology 46(20), 11289-11298.

Parameswaran, P., Torres, C.I., Lee, H.S., Krajmalnik‐Brown, R. & Rittmann, B.E. (2009), Syntrophic interactions among anode respiring bacteria (ARB) and Non‐ARB in a biofilm anode: electron balances. Biotechnology and Bioengineering 103(3), 513-523.

Reardon, K.F., Mosteller, D.C. & Rogers, J.D.B. (2000), Biodegradation kinetics of benzene, toluene, and phenol as single and mixed substrates for Pseudomonas putida F1. Biotechnology and Bioengineering 69(4), 385-400.

Ridgway, H., Safarik, J., Phipps, D., Carl, P. & Clark, D. (1990), Identification and catabolic activity of well-derived gasoline-degrading bacteria from a contaminated aquifer. Applied and environmental microbiology 56(11), 3565-3575.

Rittmann, B. (2006), The membrane biofilm reactor: the natural partnership of membranes and biofilm. Water Science & Technology 53(3), 219-225.

Rittmann, B.E. (1994), In situ bioremediation, Taylor & Francis.

Rittmann, B.E. (2007), THE MEMBRANE BIOFILM REACTOR IS A VERSA TILE PLATFORM FOR WATER AND WASTEWATER TREATMENT. Environmental Engineering Research 12(4), 157-175.

Rittmann, B.E. & McCarty, P.L. (2001), Environmental biotechnology: principles and applications, McGraw-Hill Companies, Inc, New York.

Rooney-Varga, J.N., Anderson, R.T., Fraga, J.L., Ringelberg, D. & Lovley, D.R. (1999), Microbial communities associated with anaerobic benzene degradation in a petroleum-contaminated aquifer. Applied and environmental microbiology 65(7), 3056-3063.

Sadaie, T., Sadaie, A., Takada, M., Hamano, K., Ohnishi, J., Ohta, N., Matsumoto, K. & Sadaie, Y. (2007), Reducing sludge production and the domination of Comamonadaceae by reducing the oxygen supply in the wastewater treatment procedure of a food-processing factory. Bioscience, biotechnology, and biochemistry 71(3), 791-799.

Salanitro, J.P. (1993), The role of bioattenuation in the management of aromatic hydrocarbon plumes in aquifers. Groundwater Monitoring & Remediation 13(4), 150-161.

Shim, H., Hwang, B., Lee, S.S. & Kong, S.H. (2005), Kinetics of BTEX biodegradation by a coculture of Pseudomonas putida and Pseudomonas fluorescens under hypoxic conditions. Biodegradation 16(4), 319-327.

Spain, J., Zylstra, G., Blake, C. & Gibson, D. (1989), Monohydroxylation of phenol and 2, 5-dichlorophenol by toluene dioxygenase in Pseudomonas putida F1. Applied and environmental microbiology 55(10), 2648-2652.

Spain, J.C. & Gibson, D.T. (1988), Oxidation of Substituted Phenols by Pseudomonas-Putida F1 and Pseudomonas Sp Strain-Js6. Applied and environmental microbiology 54(6), 1399-1404.

Staples, C.A., Werner, A.F. & Hoogheem, T.J. (1985), Assessment of priority pollutant concentrations in the United States using STORET database. Environmental toxicology and chemistry 4(2), 131-142.

Sublette, K.L. & Sylvester, N.D. (1987), Oxidation of hydrogen sulfide by continuous cultures of Thiobacillus denitrificans. Biotechnology and Bioengineering 29(6), 753-758.

Syron, E. & Casey, E. (2008), Membrane-aerated biofilms for high rate biotreatment: performance appraisal, engineering principles, scale-up, and development requirements. Environmental science & technology 42(6), 1833-1844.

Tang, Y., Zhou, C., Van Ginkel, S.W., Ontiveros-Valencia, A., Shin, J. & Rittmann, B.E. (2012), Hydrogen permeability of the hollow fibers used in H2-based membrane biofilm reactors. Journal of membrane science 407, 176-183.

Terada, A., Lackner, S., Tsuneda, S. & Smets, B.F. (2007), Redox‐stratification controlled biofilm (ReSCoBi) for completely autotrophic nitrogen removal: The effect of co‐versus counter‐diffusion on reactor performance. Biotechnology and Bioengineering 97(1), 40-51.

Timberlake, D.L., Strand, S.E. & Williamson, K.J. (1988), Combined aerobic heterotrophic oxidation, nitrification and denitrification in a permeable-support biofilm. Water Res 22(12), 1513-1517.

U.S. Centers for Disease Control (2007), Toxicological Profile for Benzene. http://www.atsdr.cdc.gov/toxprofiles/tp3.pdf.

U.S. Environmental Protection Agency (2009), National Primary Drinking Water Regulations. http://water.epa.gov/drink/contaminants/upload/mcl-2.pdf.

Ulrich, A.C., Beller, H.R. & Edwards, E.A. (2005), Metabolites detected during biodegradation of 13C6-benzene in nitrate-reducing and methanogenic enrichment cultures. Environmental science & technology 39(17), 6681-6691.

Ulrich, A.C. & Edwards, E.A. (2003), Physiological and molecular characterization of anaerobic benzene‐degrading mixed cultures. Environmental microbiology 5(2), 92-102.

van der Zaan, B.M., Saia, F.T., Stams, A.J., Plugge, C.M., de Vos, W.M., Smidt, H., Langenhoff, A.A. & Gerritse, J. (2012), Anaerobic benzene degradation under denitrifying conditions: Peptococcaceae as dominant benzene degraders and evidence for a syntrophic process. Environmental microbiology 14(5), 1171-1181.

Vanbriesen, J.M. & Rittmann, B.E. (2000), Mathematical description of microbiological reactions involving intermediates. Biotechnol Bioeng 68(6), 705.

Weelink, S.A.B., Eekert, M.H.A. & Stams, A.J.M. (2010), Degradation of BTEX by anaerobic bacteria: physiology and application. Reviews in Environmental Science and Bio/Technology 9(4), 359-385.

Woo, S.H. & Rittmann, B.E. (2000), Microbial energetics and stoichiometry for biodegradation of aromatic compounds involving oxygenation reactions. Biodegradation 11(4), 213-227.

World Health Organization (1993), International Program on Chemical Safety, Environmental Health Criteria 150: Benzene. http://www.inchem.org/documents/ehc/ehc/ehc202.htm.

Xie, S., Sun, W., Luo, C. & Cupples, A.M. (2011), Novel aerobic benzene degrading microorganisms identified in three soils by stable isotope probing. Biodegradation 22(1), 71-81.

Yang, H., Wang, X., Zheng, J., Wang, G., Hong, Q., Li, S., Li, R. & Jiang, J. (2013), Biodegradation of acetamiprid by Pigmentiphaga sp. D-2 and the degradation pathway. International Biodeterioration & Biodegradation 85, 95-102.

Yerushalmi, L., Lascourreges, J.-F., Rhofir, C. & Guiot, S.R. (2001), Detection of intermediate metabolites of benzene biodegradation under microaerophilic conditions. Biodegradation 12(6), 379-391.

Yu, H., Kim, B.J. & Rittmann, B.E. (2001a), The roles of intermediates in biodegradation of benzene, toluene, and p-xylene by Pseudomonas putida F1. Biodegradation 12(6), 455-463.

Yu, H., Kim, B.J. & Rittmann, B.E. (2001b), A two-step model for the kinetics of BTX degradation and intermediate formation by Pseudomonas putida F1. Biodegradation 12(6), 465-475.